Refinery Modeling

Advanced Chemical Engineering Design

Dr. Miguel J. Bagajewicz

University of Oklahoma

May 5, 2006

Aaron Smith, Michael Frow,

Joe Quddus, Donovan Howell,

Thomas Reed, Clark Landrum,

Brian Clifton

EXECUTIVE SUMMARY

This report is a refinery planning model for purchasing different crudes to meet a fixed demand while maximizing profit. The model involves 13 typical refinery processes and a blending section. Each unit has been modeled off of existing correlations, kinetic and or pilot plant data. Additional costs for increasing energy requirements were considered negligible because of the increased profit accompanied with minimal manipulations in temperature, pressure, space velocity, etc. A Visual Basic macro that uses Excel Solver was used to best estimate the purchasing requirements. Risk and uncertainty were not addressed in this initial model.

Three crudes were available for purchase from Australia, Kazakhstan, and Saudi Arabia at $71.88, $72.00, $71.20 per barrel respectively. They represent different crudes, (ie. light, sweet, sour, heavy) used in this model. The largest product demand was for regular gasoline (87 octane) at 310,000 barrels per month, with premium gasoline (91 octane) the second highest at 124,000 barrels per month. Their prices were $2.12 and $2.31 per gallon respectively. Contracts locked in specific demand amounts and included penalties for not meeting demand at 1.5 times the selling price.

Overall profit was maximized in this model, and was the objective function. The profit was a function of product sales, crude purchasing costs, and penalties for not meeting demand. The objective function was maximized by manipulation of process variables for each unit, purchasing of different crude amounts, and blending to meet product demands. Penalties for not meeting demand were significant, causing Solver to generate results that exactly met demand.

Two successful positive profit runs were completed maximizing the objective function and maintaining the constraints of each blending index. The maximum profit was $21 a barrel, with 150,000 barrels of Australia Crude, 150,000 barrels of Kazakhstan Crude, and 300,000 barrels of Saudi Arabia Crude. These values were sensitive to purchasing costs because of their similar crude properties. Future work should broaden the range of crudes used, maximize demand that changes over time, and add a wider variety of products.

Table of Contents

Introduction 6
Hydrotreating 7
Introduction and Background: 7
Purpose of model: 8
Model Development and Results: 9
Delayed Coking 12
Introduction and Background: 12
Purpose of Model: 13
Model Development and Results: 13
Catalytic Reforming 17
Introduction 17
Purpose 17
Model 18
Reaction Stoichiometry 18
Reaction Rates 19
Heat Balances 21
Results 22
Temperature Dependence 22
Pressure Dependence 23
Xylenes Isomerization 24
Introduction 24
Purpose 24
Model 24
Reaction 24
Results 24
Solvent Extraction 25
Introduction 25
Purpose 25
Model 25
Results 27
Temperature Dependence 27
Solvent to Feed Ratio Dependence 28
Visbreaker 29
Process Characteristics 29
Reaction Chemistry 30
Feed Characterization 31
Model Variables and Limitations 35
Model Equations 35
Product Groups 38

Isomerization 38
Process Characteristics 38
Reaction Chemistry 39
Catalysts 40
Feed Characterization 41
Model Variables and Limitations 42
n-Butane Model* 42
n-Pentane Model 43
n-Hexane Model* 44
Products 45
Hydrocracking 46
Introduction 46
Purpose 47
Model 48
Possible Modifications 53
Possible Alternative Models 54
Solvent Dewaxing 54
Introduction 54
Purpose 55
Model 55
Possible Modifications 57
Possible Alternative Models 57
Alkylation 57
Purpose 57
Introduction 58
Model 60
Possible Modifications 61
Polymerization 62
Purpose 62
Introduction 62
Model 63
Possible Modifications 65
Deasphalting 65
Purpose 65
Introduction 65
Asphalt 67
Deasphalted Oil (DAO) 68
Model 68
Sub critical Propane Deasphalting (Liquid-Liquid Extraction) 68
Supercritical Propane Deasphalting 71
Possible Improvements 71
Catalytic Cracking 72
Five-lump model 73
PFR 75
Blending 77
Product Blending 77

Blending Model 77
Octane Number 79
Vapor Pressure 79
Liquid Viscosity 80
Aniline Point 82
Pour Point 83
Cloud Point 83
Flash Point 84
Diesel Index and Cetane Index 85
Refinery Modeling 85
Results and Conclusions 88
Future Work 88
References 90

INTRODUCTION

Effective refinery planning is an essential part in achieving maximum profits and meeting market demands. Due to the current soaring energy prices, refineries are looking for ways to increase profits and margins. Refinery planning is a very complex problem with numerous inputs and outputs. Constantly changing market demands complicates refinery planning. The selection of which crudes to purchase is of primary importance, since different crudes yield a different palate of optimum products.

The aim of this project was to investigate each individual unit within a refinery, create a computer model of each unit, and integrate these models into a comprehensive refinery model that could be used to maximize profit for given product demands. Each unit is modeled using correlated data or theoretical equations so that for any given feed the products of the unit can be estimated. The intermediate streams within the refinery must first be characterized by specific properties that are important for the prediction of products for the unit that they feed.

A refinery is composed of as many as thirty or more processes that are both in series and parallel of each other. A change in one process will inevitably affect all other processes down the line. Due to the complex nature of the reactions and separations that take place in these processes, modeling them can be difficult at best. Various methods are in place to estimate yields of products that come from these units. Yield estimates come from previous operational data, experimentation, correlations, kinetic modeling, etc. Among these methods kinetic modeling typically yields the most accurate results but requires a lot of information about the reactions that take place with in the units. Since crude oil contains thousands of different hydrocarbon compounds and other impurities, modeling reactions on the molecular level is near impossible.

One method of modeling is the use of pseudo components instead of individual species. Pseudo components are groups of compounds that have been lumped together based on a range of a particular property. Specific properties that can define a lumped parameter are: the boiling point curve, K_w factor, molecular weight, etc. Therefore, with many parameters to choose from, the refinery model used the boiling point curve to determine the cuts of the crude. This was done

mainly because the boiling point can provide an accurate representation of the molecular weight of the species, as well as group the products into a relatively narrow range.

A simplified refinery was considered for the scope of this project. An individual input/output model was developed for each of the major refinery units. These models were then connected into a comprehensive refinery model that had three crude inputs, 26 operating parameters, and 7 outputs or products. The profit for a specific set of operating conditions, feeds, and products was calculated for the overall refinery model. The model consisted of 13 units: hydrotreating, delayed coking, catalytic reforming, xylenes isomerization, solvent extraction, visbreaking, isomerization, solvent dewaxing, alkylation, polymerization, deasphalting, catalytic cracking, and blending.

HYDROTREATING

INTRODUCTION AND BACKGROUND:

Sulfur content in gasoline and diesel are now seeing new regulations for lower content. In particular, refineries are expected to be producing diesel with 15 ppm sulfur or less by June of 2006.[1] The processes that refineries utilize to remove sulfur is a form of hydrotreating. Not only does hydrotreating remove sulfur from hydrocarbons, but it also removes nitrogen from hydrocarbons and decreases the aromatic in a given feed. The reactions for sulfur and nitrogen removal are carried out in similar fashion. For the removal of aromatics, hydrogen is added to the aromatic ring to increase the saturation of the molecule, which eliminates the double bonds to produce napthenes. An example of sulfur removal can be seen below in Figure 1.

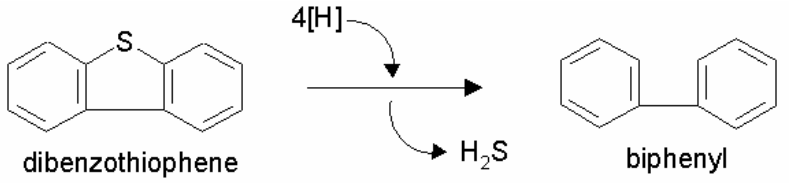

Figure 1: Sulfur Removal[2]

Hydrotreating takes place in a packed bed reactor. The feed stream from the distillation column is mixed with a hydrogen stream and heated prior to entering the reactor. This vapor mixture then flows through the reactor where the sulfur compounds, nitrogen compounds, and hydrogen molecules adsorb onto the surface of the catalyst and react with one another. Leaving the reactor is the treated product along with byproducts of the reaction such as H_2S and NH_3. These byproducts are partially removed by the condensation of the exiting stream. They are completely removed after flowing through the distillation column at the end of the hydrotreating process. The process flow diagram for this process can be seen below in Figure 2.

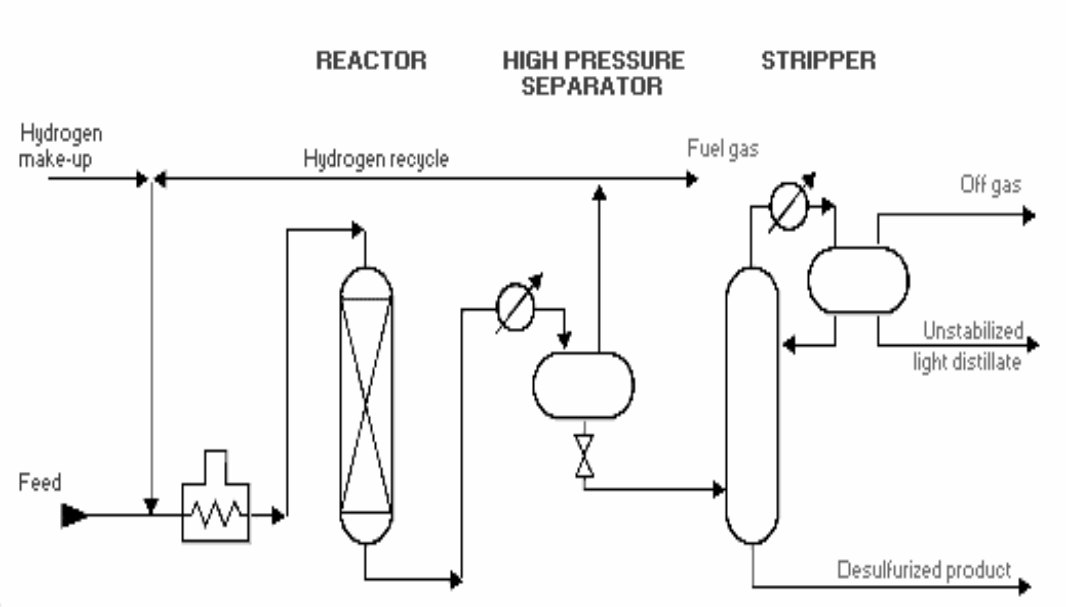

Figure 2: Hydrotreating Unit PFD[3]

PURPOSE OF MODEL:

The purpose of the model that was developed for hydrotreating is to predict the amount of sulfur, nitrogen, and aromatic compounds remaining in the stream exiting the reactor given their initial concentrations within the feed. It is also desired that the model account for the effects of changing reaction temperature, reaction pressure, hydrogen to hydrocarbon ratio, and weight of catalyst.

MODEL DEVELOPMENT AND RESULTS:

Hydrotreating occurs for three fractions which are separated in the distillation column. These are the napthenes, middle distillates, and gas oils. For each of the feeds the reaction conditions are slightly different.

In work performed by Galiasso[4] there were reaction orders for the removal of sulfur and nitrogen containing compounds as well as aromatics. They determined that for molybdenum cobalt (MoCo) the orders were as shown in the table below.

Table 1: Reaction Orders[5]

Reaction	Hydrocarbon Order	Hydrogen Order
Sulfur Removal	2.00	0.75
Nitrogen Removal	1.40	0.60
Basic Nitrogen Removal	1.20	0.50
Aromatic Saturation	1.00	1.00

They also determined the activation energies for the each of the reactions as shown in Table 2.

Table 2: Activation Energies[6]

Reaction	Activation Energy (kcal/mol)
Sulfur Removal	25
Nitrogen Removal	20
Basic Nitrogen Removal	20
Aromatic Saturation	25

Using these values makes it is possible to determine the kinetic equations, which describe the removal of sulfur, nitrogen, and aromatics in the packed bed reactor. These equations show the rate of removal of the components based on their concentrations.

$$r_s = \frac{dC_S}{dW} = k_s C_s^{\ 2} C_{H_2}^{\ .75}$$ **Eq. 1**

$$r_N = \frac{dC_N}{dW} = k_N C_N^{\ 1.4} C_{H_2}^{\ .6}$$ **Eq. 2**

$$r_{BN} = \frac{dC_{BN}}{dW} = k_{BN} C_{BN}^{\ 1.2} C_{H_2}^{\ .5}$$ **Eq. 3**

$$r_{Ar} = \frac{dC_{Ar}}{dW} = k_{Ar} C_{Ar} C_{H_2}$$ **Eq. 4**

Also, since the activation energies are given the following equations are valid.

$$k_S = A_S e^{\frac{-E}{RT}} = A_S e^{\frac{-25 kcal/mol}{RT}}$$ **Eq. 5**

$$k_N = A_N e^{\frac{-E}{RT}} = A_N e^{\frac{-20 kcal/mol}{RT}}$$ **Eq. 6**

$$k_{BN} = A_{BN} e^{\frac{-E}{RT}} = A_{BN} e^{\frac{-20 kcal/mol}{RT}}$$ **Eq. 7**

$$k_{Ar} = A_{Ar} e^{\frac{-E}{RT}} = A_{Ar} e^{\frac{-25 kcal/mol}{RT}}$$ **Eq. 8**

With these equations the hydrotreating process can be simulated. The only variable that would not be available from the data for the inlet feed are the Arrhenius constants for each of the reactions. Fortunately, data was available from the experiments they carried out, which enabled the Arrhenius constants to be estimated. Also, it was assumed that the concentrations could be estimated using the ideal gas law. The values in Table 3 were used as the equivalent mole fractions. Their corresponding product yields from the reactions can be seen in Table 4. Another piece of information, which was necessary in order to determine the Arrhenius constants, was the column specifications and mass of catalyst used in prototype process.

Table 3: Experimental Feed Conditions[7]

Feed Properties:	
Sulfur (ppm)	4500
Nitrogen (ppm)	350
Basic Nitrogen (ppm)	180
Aromatic %	50
Density	0.8730
Molecular Weight	200

Table 4: Reaction Condition and Results[8]

Operating Conditions:							
Temperature (^oC)	370	370	370	370	370	350	390
Pressure (psig)	50	50	50	80	30	50	50
LHSV (h^{-1})	3.0	1.5	1.0	1.5	1.5	3.0	3.0
H_2/HC	200	200	200	200	200	200	200

Product Analysis:							
Sulfur (ppm)	110	45	35	33	66	214	70
Nitrogen (ppm)	130	85	63	68	108	150	110
Basic Nitrogen (ppm)	75	45	34	38	54	115	44
Aromatic %	36	30	38	25	34	37	32
Density	0.8682	0.8615	0.8605	0.8610	0.8645	0.8675	0.8633
Molecular Weight	212	187	180	181	214	200	185

Through trial and error of varying the Arrhenius constants for each of the equations a good estimate was determined.

Table 5: Estimated Arrhenius Constants

A_S	A_N	A_{BN}	A_{Ar}
1.33E+06	6.00E+01	4.50E+01	6.00E+01

DELAYED COKING

INTRODUCTION AND BACKGROUND:

Delayed coking is a process used by refineries to form a valuable product out of the typically unusable bottoms from the vacuum distillation column. The products that are formed from this process are gas, napthenes, gas oil, and coke.

The process that produces these valuable products is semi-continuous. The feed from the bottom of the column is heated in a furnace and then fed into multiple coking drums. It is then held in the drums for long lengths of time and maintained at high temperatures. This process breaks down the molecules into the four products mentioned above. After the reaction has taken place, the products are fed into the fractionator, which separates the different components produced. The process flow diagram below shows this process.

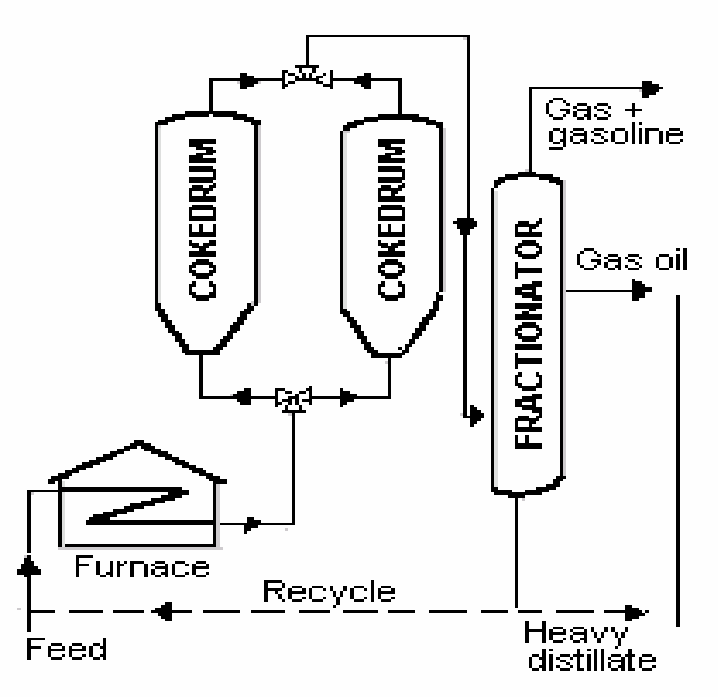

Figure 3: Delayed Coking PFD

PURPOSE OF MODEL:

The purpose of the model for this unit is to predict the amount of gas, napthenes, gas oil, and coke produced in this process, given the properties of the inlet feed. It is also desired to predict the effect of pressure on the final products produced.

MODEL DEVELOPMENT AND RESULTS:

The basis of the model that was used for this process comes from Gary and Handwerk[9]. They develop equations in which the yield of coke, gas, gas oil, and napthenes are estimated based on the Conradson Carbon Residue. These equations are shown below.

Coke wt % = 1.6 x CCR **Eq. 9**

Gas (C_4-) wt % = 7.8 + (0.144 x CCR) **Eq. 10**

Napthenes wt % = 11.29 + (0.343 x CCR) **Eq. 11**

Gas oil wt % = 100 – Coke wt % – Gas wt % - Napthenes wt % **Eq. 12**

The assumption in this estimate of the products of delayed coking is that the actual processing conditions of delayed coking have little factor in the products that are produced. This is actually a reasonable assumption given the severity of the process with the main goal of thermally cracking the heavy bottom distillates. Typically[10], operating temperatures of delayed coking range from 1095 to 1260°C. The temperatures coupled with the fact that the feed remains in the coking drum for up to 24 hours explain why equilibrium is assumed versus kinetics.

Though their model did not account for the effect of pressure on the process it does have an effect on the products coming out of the process. This can be seen in the table below.

Table 6: Effect of Pressure on Coking Product[11]

	CCR (wt %)	18.1	
	Correlation	15 psig	35 psig
Coke	29	27.2	30.2
Gas Yield	10.4	9.1	9.9
Napthenes Yield	17.5	12.5	15
Gas Oil Yield	43.1	51.2	44.9

It can be seen that the correlation is able to predict the amounts of each of the products; however the correlation significantly deviates from the experimental data. Therefore, by modification of the original Gary and Handwerk[12] equations a new correlation was created.

To develop the new correlation the difference between the 15 psig process and the 35 psig process was compared. This difference is shown in the table below.

Table 7: Change Due to Pressure

	15 psig	35 psig	Change	Percentage Change
Coke	27.2	30.2	**3**	**11.0**
Gas Yield	9.1	9.9	**0.8**	**8.8**

Napthenes Yield	12.5	15	**2.5**	**20.0**
Gas Oil Yield	51.2	44.9	**-6.3**	**-12.3**

Now it is assumed that this change in production is linear between the two pressures. This linear assumption leads to the following pressure adjustment factors, which will be added two each of the equations.

Coke:

$$Factor = 3 \times \frac{(P-15)}{20} \qquad \textbf{Eq. 13}$$

Gas:

$$Factor = .8 \times \frac{(P-15)}{20} \qquad \textbf{Eq. 14}$$

Napthenes:

$$Factor = 2.5 \times \frac{(P-15)}{20} \qquad \textbf{Eq. 15}$$

Assuming these linearizations' are valid, the Factors show the effect of pressure on the final products. Now it is possible to add these into the original Gary and Handwerk[13] equations to determine the overall products. Unfortunately, as Table 6 shows the correlation does not replicate the values at 15 psig. Therefore, the constants in these equations were normalized to fit the value at 15 psig. It was important not to change each value by too much and risk skewing the affect CCR in the feed had on the products. The new equations found using this method are shown below.

$$\text{Coke wt \%} = 1.5 \text{ x CCR} + 3 \times \frac{(P-15)}{20} \quad \textbf{Eq. 16}$$

$$\text{Gas } (C_4\text{-}) \text{ wt \%} = 7.4 + (0.1 \text{ x CCR}) + .8 \times \frac{(P-15)}{20} \quad \textbf{Eq. 17}$$

$$\text{Napthenes wt \%} = 10.29 + (0.2 \text{ x CCR}) + 2.5 \times \frac{(P-15)}{20} \quad \textbf{Eq. 18}$$

$$\text{Gas oil wt \%} = 100 - \text{Coke wt \%} - \text{Gas wt \%} - \text{Naptha wt \%} \quad \textbf{Eq. 19}$$

Table 8: Correlation with Pressure

	CCR (wt%)	18.1		
	Correlation (15 psig)	Correlation (35 psig)	15 psig	35 psig
Coke	27.2	30.2	27.2	30.2
Gas Yield	9.2	10	9.1	9.9
Napthenes Yield	13.9	16.4	12.5	15
Gas Oil Yield	49.7	43.4	51.2	44.9

CATALYTIC REFORMING

INTRODUCTION

Catalytic reforming seeks to increase the octane number of naptha distillation cuts by converting napthenes and paraffins into aromatics, light end hydrocarbons (C_1 – C_5), and hydrogen. The reactions take place in packed bed reactors at high temperatures (900 ºF – 950 ºF) and pressures (30 atm – 40 atm) while flowing over a platinum bi-function catalyst on an alumina support. Reactions are further facilitated by large hydrogen partial pressures through a recycle stream.

PURPOSE

The purpose of this model is to predict the output of the reactor system through a series of simplified inputs. While more than a hundred individual species enter the system, we divide them into 3 categories for simplification of reaction stoichiometry and kinetic parameters. The three categories defined are paraffins, napthenes, and aromatics. Paraffins are mostly straight chain hydrocarbons, such as n-octane or iso-heptane, with the highest hydrogen to carbon ratios of the three groups. Napthenes are typically cyclic hydrocarbons, such as cyclohexane or methylcyclopentane, with slightly lower hydrogen to carbon ratio than paraffins. Aromatics are cyclic hydrocarbons, such as benzene or para-xylene, with the lowest hydrogen to carbon ratio of the three groups.

Predicting the change in reactants to products allows one to predict what sort of products will be available in the refinery for sale. Aromatics have relatively large research and motor octane numbers (RON & MON) and are typically blended with other components in premium gasoline, fractionated and sold as solvents, or isomerized and sold as chemical feed stocks. Paraffins are typically isomerized into branched hydrocarbons with higher RON & MON values. There is not a large demand for napthene products currently and it is desired to reduce the amount of them into more valuable products.

MODEL

The model utilizes lumped parameters for pseudo-components to predict the reaction stoichiometry, reaction rates, and heat balances. Each of these series of equations was published by Rase in 1980.

Reaction Stoichiometry

Figure A: Lumped Reaction Stoichiometry

$$\boxed{\begin{array}{l}(1) Napthenes \longleftrightarrow aromatics + 3 * H_2 \\ (2) Paraffins \longleftrightarrow napthenes + H_2 \\ (3) Hydrocracking\_of\_paraffins \\ (4) Hydrocracking\_of\_napthenes\end{array}}$$

Source [Case 108 - Catalytic Reforming]

Reaction (1) – Conversion of napthenes to aromatics

$$\boxed{C_nH_{2n} \longleftrightarrow C_nH_{2n-6} + 3H_2}$$

Source [Case 108 - Catalytic Reforming]

Reaction (2) – Conversion of paraffins to napthenes

$$\boxed{(2) C_nH_{2n+2} \longleftrightarrow C_nH_{2n} + H_2}$$

Source [Case 108 - Catalytic Reforming]

Reaction (3) – Hydrocracking of parffins

$$\boxed{C_nH_{2n+2} + \left(\frac{n-3}{3}\right)H_2 \longrightarrow \frac{n}{15}C_1 + \frac{n}{15}C_2 + \frac{n}{15}C_3 + \frac{n}{15}C_4 + \frac{n}{15}C_5}$$

Source [Case 108 - Catalytic Reforming]

Reaction (4) – Hydrocracking of napthenes

$$C_nH_{2n} + \frac{n}{3}H_2 \longrightarrow \frac{n}{15}C_1 + \frac{n}{15}C_2 + \frac{n}{15}C_3 + \frac{n}{15}C_4 + \frac{n}{15}C_5$$

Source [Case 108 - Catalytic Reforming]

Reaction Rates

Reaction (1) – Conversion of napthenes to aromatics

Equilibrium for Reaction (1)

$$K_{P1} = \frac{P_A * P_H^3}{P_N} = \exp\left(46.15 - \frac{46045}{T}\right), [=] atm^3$$

Source [Case 108 - Catalytic Reforming]

Kinetic constant for Reaction (1)

$$\hat{k}_{P1} = \exp\left(23.21 - \frac{34750}{T}\right), [=] \frac{moles}{(hr)(lb\_cat.)(atm)}$$

Source [Case 108 - Catalytic Reforming]

Reaction rate for Reaction (1)

$$-\hat{r}_1 = \hat{k}_{P1}\left(P_N - \frac{P_A * P_H{}^3}{K_{P1}}\right)[=] \frac{moles\_napthene\_converted\_to\_aromatics}{(hr)(lb\_cat.)}$$

Source [Case 108 - Catalytic Reforming]

$$\left(-\hat{r}_1\right)\left(\frac{\Delta W}{F_T}\right) = \Delta X_1$$

Source [Case 108 - Catalytic Reforming]

Reaction (2) – Conversion of napthenes to paraffins

Equilibrium for Reaction (2)

$$K_{P2} = \frac{P_P}{P_N * P_H} = \exp\left(\frac{8000}{T} - 7.12\right), [=] atm^{-1}$$

Source [Case 108 - Catalytic Reforming]

Kinetic constant for Reaction (2)

$$\hat{k}_{P2} = \exp\left(35.98 - \frac{59600}{T}\right), [=] \frac{moles}{(hr)(lb\_cat.)(atm)^2}$$

Source [Case 108 - Catalytic Reforming]

Reaction rate for Reaction (2)

$$-\hat{r}_2 = \hat{k}_{P2}\left(P_N * P_H - \frac{P_P}{K_{P2}}\right)[=] \frac{moles\_napthene\_converted\_to\_paraffins}{(hr)(lb\_cat.)}$$

Source [Case 108 - Catalytic Reforming]

$$\left(-\hat{r}_2\right)\left(\frac{\Delta W}{F_T}\right) = \Delta X_2$$

Source [Case 108 - Catalytic Reforming]

Reaction (3) – Hydrocracking of paraffins

Kinetic constant for Reaction (3)

$$\hat{k}_{P3} = \exp\left(42.97 - \frac{62300}{T}\right), [=] \frac{moles}{(hr)(lb\_cat.)}$$

Source [Case 108 - Catalytic Reforming]

Reaction rate for Reaction (3)

$$-\hat{r}_3 = \hat{k}_{P3}\left(\frac{P_P}{P}\right)[=] \frac{moles\_paraffins\_converted\_by\_hydrocracking}{(hr)(lb\_cat.)}$$

Source [Case 108 - Catalytic Reforming]

$$\left(-\hat{r}_3\right)\left(\frac{\Delta W}{F_T}\right) = \Delta X_3$$

Source [Case 108 - Catalytic Reforming]

Reaction (4) Hydrocracking of napthenes

Kinetic constant for Reaction (4)

$$\hat{k}_{P4} = \exp\left(42.97 - \frac{62300}{T}\right), [=] \frac{moles}{(hr)(lb\_cat.)}$$

Source [Case 108 - Catalytic Reforming]

Reaction rate for Reaction (4)

$$-\hat{r}_4 = \hat{k}_{P4}\left(\frac{P_N}{P}\right)[=] \frac{moles\_napthenes\_converted\_by\_hydrocracking}{(hr)(lb\_cat.)}$$

Source [Case 108 - Catalytic Reforming]

$$\left(-\hat{r}_4\right)\left(\frac{\Delta W}{F_T}\right) = \Delta X_4$$

Source [Case 108 - Catalytic Reforming]

Heat Balances

$$\Delta W\left[\left(-\hat{r}_1\right)\left(-\Delta H_1\right)(3) + \left(-\hat{r}_2\right)\left(-\Delta H_2\right) + \left(-\hat{r}_3\right)\left(-\Delta H_3\right)\left(\frac{n-3}{3}\right) + \left(-\hat{r}_4\right)\left(-\Delta H_4\right)\left(\frac{n}{3}\right)\right] = \Sigma \Im_j C_{Pj} \Delta T$$

Source [Case 108 - Catalytic Reforming]

$$Q = \dot{n} * C_{P,Molar} * \Delta T$$

The equations were entered into Excel and calculated using a differential method of integration with changeable input parameters. The following parameters are changeable in this model:

APIº - API gravity of cut entering system

ASTM D86 distillation curve

TBP distillation curve

F_C – total molar flow rate

n_P- mole % of paraffins entering system

n_N- mole % of napthenes entering system

n_A- mole % of aromatics entering system

$C_{P,Fresh\ \&\ Recycle}$ – for cut entering system and for the recycle stream

H_2/F_C – ratio of recycled hydrogen to fresh feed

n_H- mole % of hydrogen in recycle stream

C_1/C_3- ratio of methane to propane in recycle stream

C_2/C_3- ratio of ethane to propane in recycle stream

T_R- temperature that process stream enters each reactor

T_A- approach temperature that primary heat exchanger reaches between feed and product streams

$D_{1,2,3}$- diameter of reactors 1, 2, & 3

$v_{1,2,3}$- velocity of gas entering reactors 1, 2, & 3

$W_{1,2,3}/F_C$ – ratio of catalyst weight in reactors 1, 2, & 3 to fresh feed molar flow rate

RESULTS

The output of the model indicated many factors go into changing the possible output. It was determined that two paramaters, temperature and pressure, were the easiest to change in an actual refinery without changing equipment. As such, the effect of changing each of these parameters is discussed in detail.

Temperature Dependence

Increasing temperature increases both the rate constant of the reactions and the equilibrium constant. As the overall reactions are endothermic, an increase in inlet temperature raises the outlet temperature. Thus, desired reaction rates have higher values over the length of the reactor. This equates to a greater concentration of aromatics in the product stream and a smaller concentration of napthenes. This trend is shown in **Figure A**.

Figure A

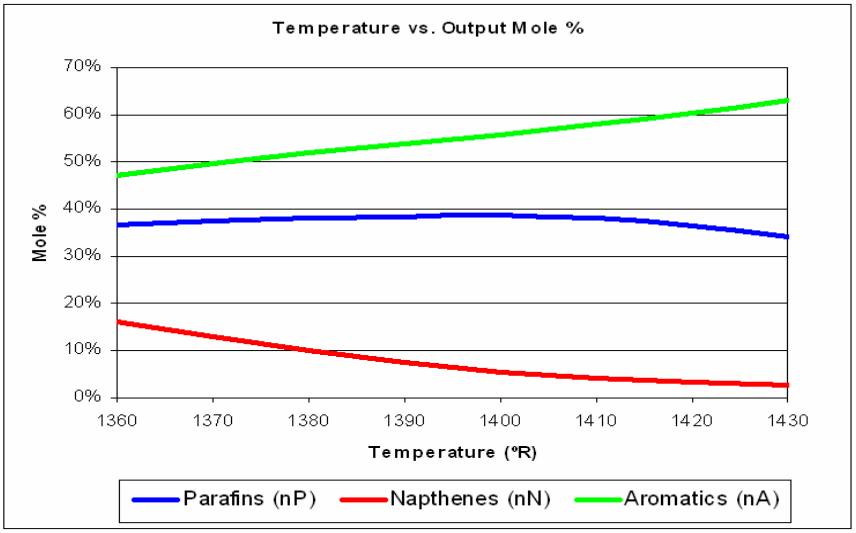

Pressure Dependence

Increasing total pressure decreases the overall reaction rates for the hydrocracking reactions. This means there is less generation of lighter hydrocarbons and hydrogen generated from hydrocracking of napthenes. This increases the final concentration of napthenes in the product stream. This trend is shown in **Figure B**.

Figure B

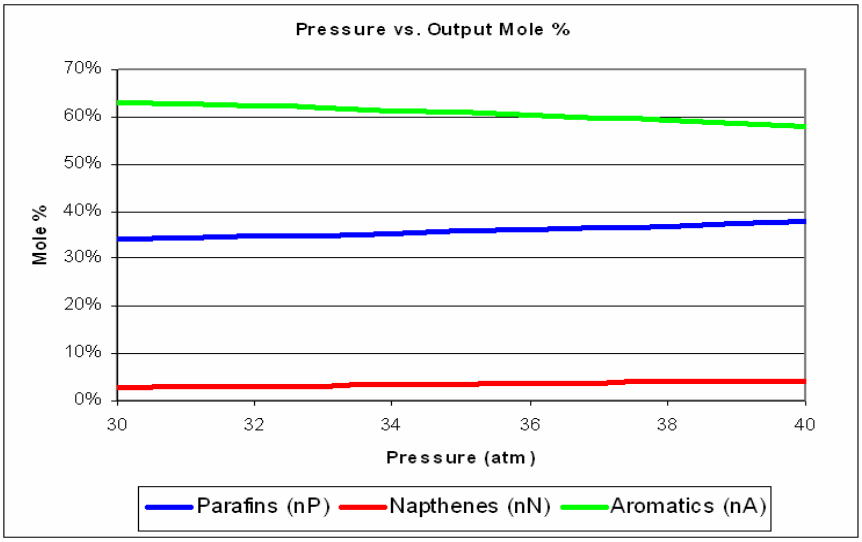

XYLENES ISOMERIZATION

INTRODUCTION

Xylenes isomerization seeks to change less valuable C_8 aromatics into more valuable aromatics. Mixed xylenes react to form an equilibrium distribution which is followed by the removal of valuable aromatics with the remainder recycled back to the reactor for re-equilibration. The equilibrium distributions of the C8 aromatics are controlled by temperature.

PURPOSE

This model seeks to predict the amount and distribution of C_8 aromatics output from an isomerization reactor. The reaction is driven by equilibrium and is assumed to react rapidly. There was no readily available kinetic rate data for the reaction. After reacting, the valuable ortho- and para- xylenes are separated along with the ethylbenzene while the meta-xylenes are recycled to the reactor. Additional recycling of ortho-xylene and ethylbenzene occurs when market prices and demand do not make selling of them economic.

MODEL

The model is an adaptation of a graph from the Kirk-Othmer Encyclopedia of Chemical Technology – 4th Edition Supplement. The reaction is simply conversion between the different C_8 aromatic isomers.

Reaction

$$m-Xylene \longleftrightarrow o-Xylene \longleftrightarrow p-Xylene \longleftrightarrow EthylBenzene$$

RESULTS

By changing the temperature in the reactor, the output ratio of products is changed.

Figure C

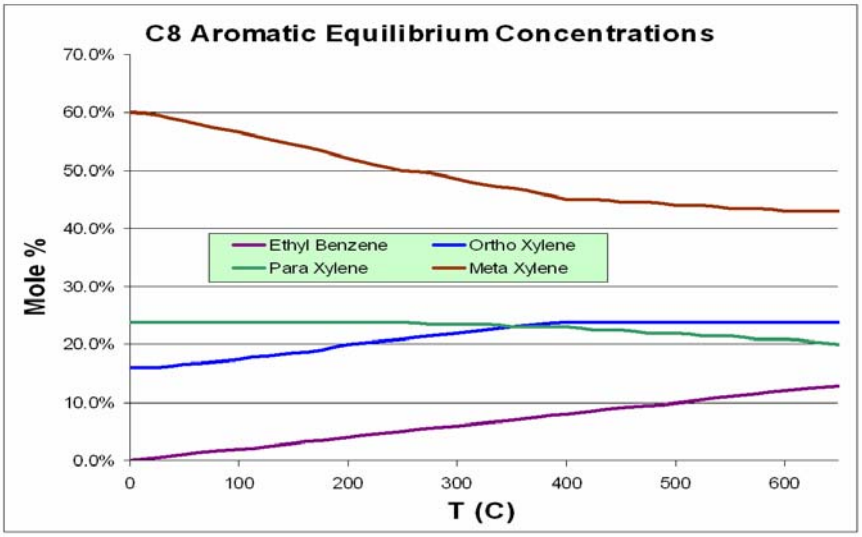

SOLVENT EXTRACTION

INTRODUCTION

Solvent extraction seeks to remove high octane number aromatics from lube oils to increase the viscosity index. Solvents selectively extract aromatics over paraffins in a liquid – liquid extraction column with agitation. The selectivity and extraction power is influenced by the solvent to feed ratio, extraction temperature, and agitator speed.

PURPOSE

The purpose of this model is to predict the amount of aromatics (extract) extracted from lube oil base stock (raffinate). This was estimated by using average K (equilibrium extraction constant) values taken from Perry's Chemical Engineering Handbook. The K values are then placed into an extraction coefficient equation given in Seader & Henley's Separations Process Principles. It also predicts the amount of raffinate lost in the extract stream and the purity of the extracted raffinate.

MODEL

The K values were taken for these general extraction cases:

1. Aromatics extracted from a napthene with furfural

2. Aromatics extracted from a paraffin with furfural
3. Larger aromatics extracted from a larger paraffin with furfural

These are detailed in **Figure D**

Figure D

Source [Perry's Chemical Engineers Handbook 7th Ed. - Table 15-5]						
Modeled as an average ternary extraction of the following						
Carrier (A)	Solute (B)	Solvent (S)	T (°C)	T (°R)	K (Y/X)	
Cyclohexane	Benzene	Furfural	25	536.4	0.680	
iso-octane	Benzene	Furfural	25	536.4	0.833	
docosane	1,6-diphenylhexane	Furfural	25	536.4	0.79	Extrapolated
			45	572.4	0.98	
			80	635.4	1.1	
			115	698.4	1.062	
			Average K @ 536°R (25°C)		0.767	

The temperature dependence is taken from the 3rd general extraction case as it was the only one that had K values for different temperatures. A parabola was fitted to the data and moved to the point of the average K value for all three extraction cases at 25ºC. The parabola that describes the temperature dependence is:

$$K = T^2(-2E5) + 0.0259 * T - 7.371$$

By changing the temperature and the solvent to feed (S/F) ratio, determination of the extraction coefficient (E) is possible.

$$E = K * \frac{S}{F}$$

The percentage extracted is based on the number of equilibrium stages (n) and the extraction coefficient given as follows:

$$\%Extracted = 1 - \frac{1}{\sum_{n=0}^{N} E^n}$$

The solvent to feed ratio also affects the specific gravity and the %yield of the raffinate. Data was taken from the Petroleum Refining 2 – Separation Processes by Wauquier in order to determine these effects. The data is given in **Figure E**.

Figure E

93 wt% Furfual Solvent		
Solvent to Feed Ratio	Raffinate Yield	Raffinate Specific Gravity
0	100%	0.925
3	75%	0.900
6	63%	0.895
9	53%	0.892
12	47%	0.891

A line was fit to the raffinate yield percentage and given as follows:

$$RaffinateYield\% = \left(\frac{S}{F}\right) * (-0.0426) + 0.9318$$

A parabola was fit to the specific gravity yield and adjusted to go through the input specific gravity which is the last term in the equation.

$$RaffinateS.G. = \left(\frac{S}{F}\right)^2 * (0.0004) - \left(\frac{S}{F}\right) * (0.0073) + 0.9229$$

RESULTS

Temperature Dependence

Increasing the temperature of the extraction directly increases the amount of solute the solvent can hold. Unfortunately, increasing the temperature also decreases the selectivity of the solvent towards the aromatic compounds. This model, however, cannot account for this fact due to the limited thermodynamic data. The general trend without selectivity issues is shown in **Figure F**

Solvent to Feed Ratio Dependence

Increasing the solvent to feed ratio creates a more pure raffinate stream at the cost of a smaller recovery of the raffinate. Additionally, increasing the solvent to feed ratio decreases the purity of the extract. This general trend is shown in **Figure G**.

Figure F

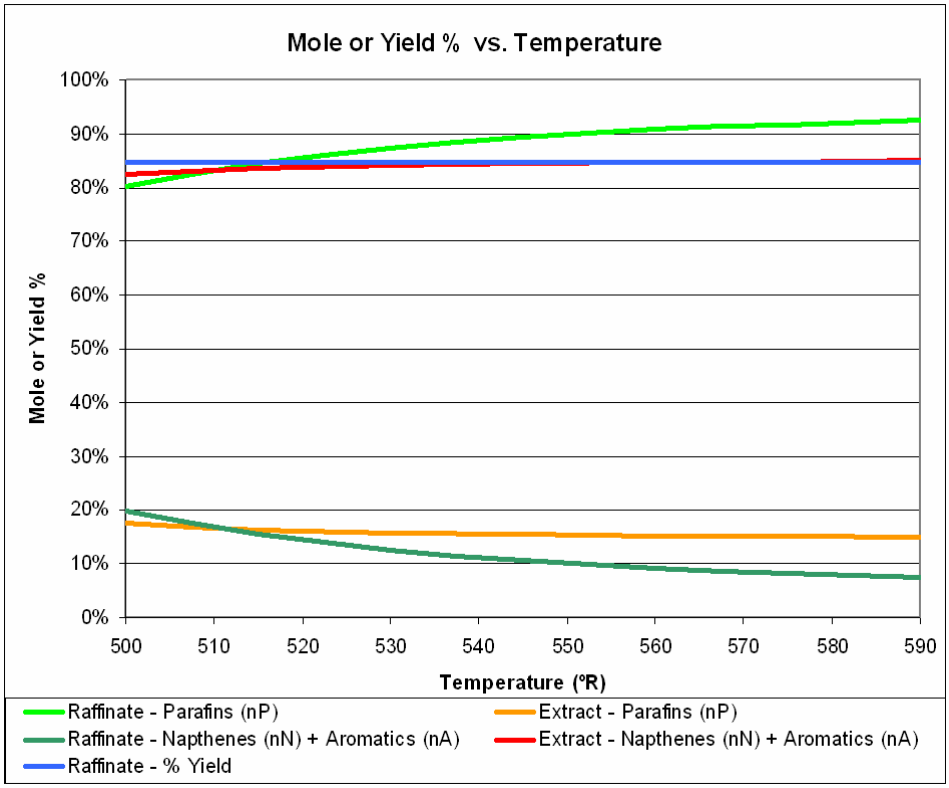

Figure G

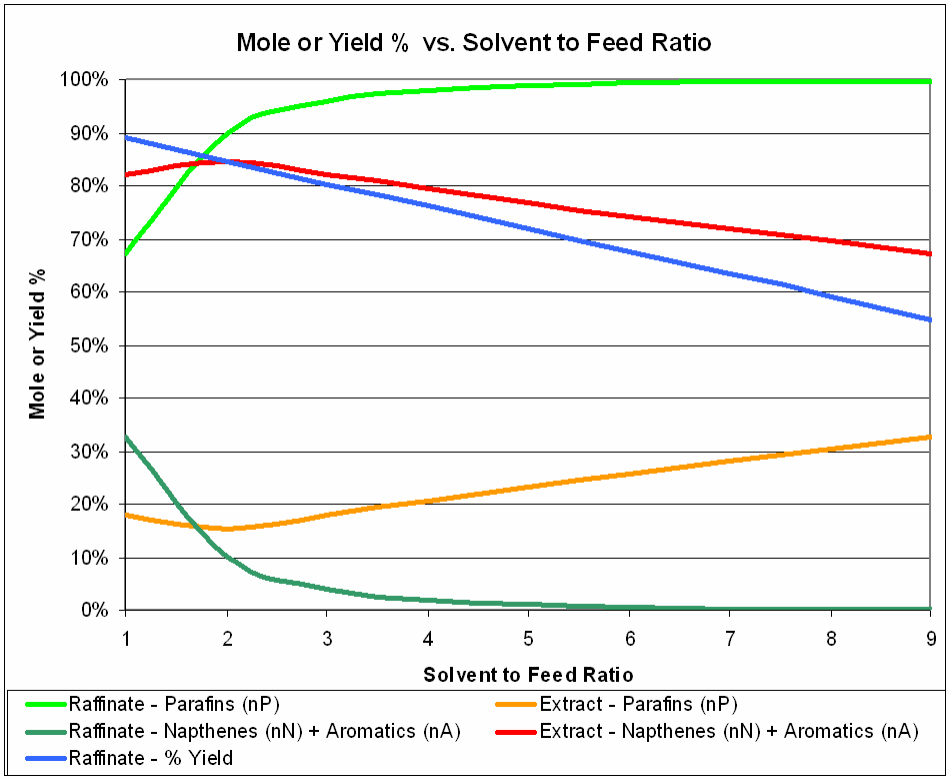

VISBREAKER

Visbreaker design typically consists of one or more furnaces that heat either atmospheric or vacuum residue to a temperature at which the residue spontaneously cracks into lighter components. This cracking of the residue produces some lighter distillates- gas and gasoline- while substantially reducing the viscosity of the residue[14]. Typically atmospheric residue is cracked to maximize the light and middle distillates; vacuum residues are cracked to reduce the viscosity such that the crude can be used as an industrial fuel oil[15]. The cracking reaction is mainly dependent on the temperature and residence time of the unit; thus these variables are also the manipulated variables in the process model. The unit is modeled as a plug flow reactor, with first order kinetics based on molar concentrations of the feed components.

PROCESS CHARACTERISTICS

Two basic designs of visbreaking units are used in industry. One design consists of the process stream flowing through a heated coil in which the reaction takes place[16]. After the process stream leaves the furnace coil the reaction is quenched with a either cold gas oil or residue[17].

This design is essentially a high temperature, short residence time unit. The other design uses a soaking drum to increase the residence time of the process. The addition of a soaking drum allows the process to run at lower temperatures since the extent of the reaction is kept constant through increased exposure to the lower temperature[18].

Typically the furnace outlet temperature varies between 430 and 490^{o}C depending on the unit and feed characteristics, such as having a soaking section. Pressure is only a concern in as much that the feed does not vaporize. Typically, a pressure of 5 to 12 bar, is enough to maintain a liquid phase. The products of the reaction are then separated into either gas (C_1-C_4), gasoline (C_5-165^{o}C), gas oil (165-350^{o}C), or residue (350^{o}C +)[19].

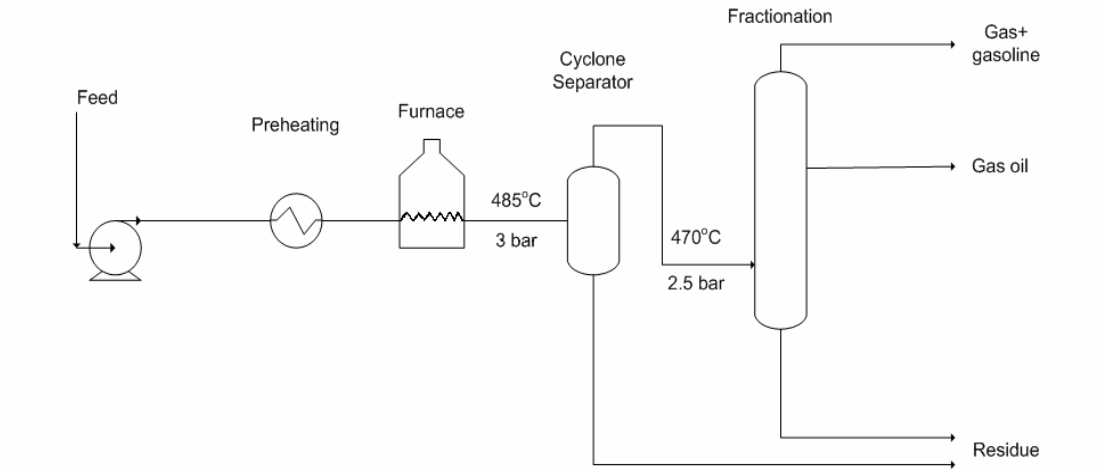

Figure 4: Typical visbreaker -no soaker

REACTION CHEMISTRY

The reaction that takes place in a visbreaker is a spontaneous reaction at the elevated temperatures of the unit. As the temperature in the unit increases the carbon chains begin to break down producing shorter carbon chains reducing the viscosity of the residue. Typical the conversion for the visbreaking reaction is limited to between 10 to 50% depending on the unit conditions[20].

For the model, the number of reactions that take place in the visbreaker is dependent on the number of components in the feed. For n=45 there are (n-2)(n-1)/2 or 946 reactions total. Each of these reactions is taken into account in the model. For each of the i-components there is (i-2)(i-1)/2 parallel reactions paths that are possible. S_i is a lumped parameter containing every carbon compound with the number of carbons equal to i. O_i is the same as s_i except with a higher degree of unsaturation[21]. This distinction between s_i and o_i comes from the visbreaking reaction being a hydrogen deficient reaction. When the carbon chains crack, only enough hydrogen is present for one of the product chains to be completely saturated[22]. The reaction pathway of each s_i component can be seen in figure 5.

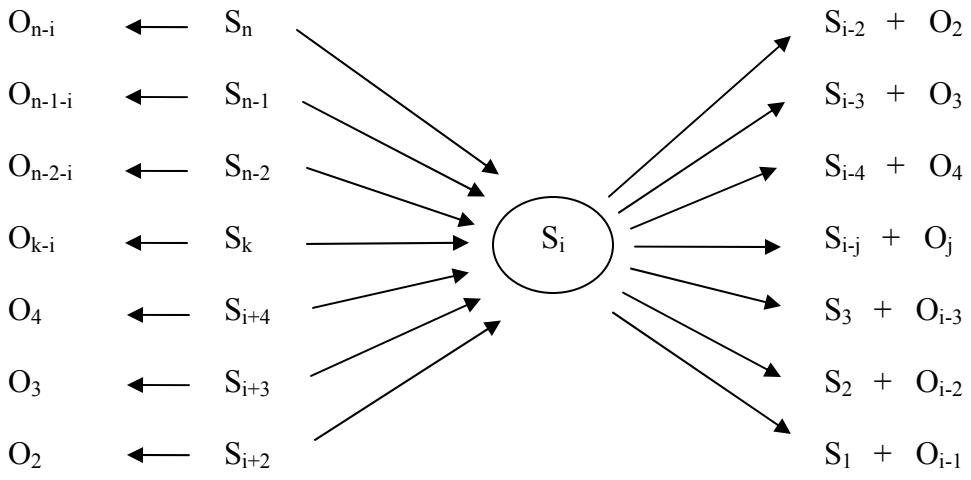

Figure 5: Reaction Pathways for every S_i compound[23]

The component s_i is formed from each component equal to and greater than s_{i+2}. Each of these cracking reactions of the s_{i+2} and greater components also produces the corresponding o_2 to o_{n-i} products. The component s_i cracks into each component s_{i-2} and smaller while simultaneously producing the o_2 to o_{i-1} products.

FEED CHARACTERIZATION

The visbreaker feed is either an atmospheric or vacuum residue. Typically the atmospheric residue is used when maximizing the light distillates of the refining process. Vacuum residues are processed to reduce their viscosity to the point where they can be used as industrial fuel oils.

The feed for the model must be in the form of concentrations of each s_i component. However the two feeds given with the model are supplied in the form of true boiling point (TBP) cuts with weight percents-table 9. Therefore, an estimation of the each carbon number's concentration was found[24].

Table 9: TBP Cuts for Atmospheric Residue used in the model[25]

Cut	TBP, ^{0}C	ρ, g/cm3	Mol. Weight	wt%
1	58.61	0.6987	84	0.000155
2	72.50	0.7020	91	0.000167
3	86.39	0.7112	98	0.000358
4	100.28	0.7200	104	0.000574
5	114.17	0.7296	111	0.000817
6	128.06	0.7403	117	0.001306
7	141.94	0.7511	126	0.002071
8	155.83	0.7613	134	0.002699
9	169.72	0.7740	142	0.005719
10	183.61	0.7891	150	0.009071
11	197.50	0.8001	158	0.009854
12	218.33	0.8137	172	0.042647
13	246.11	0.8321	192	0.088564
14	273.89	0.8494	214	0.229895
15	301.67	0.8625	239	0.331273
16	329.44	0.8744	266	0.853469
17	357.22	0.8875	274	1.601796
18	398.89	0.9040	341	6.041235
19	454.44	0.9255	410	10.215256
20	510.00	0.9500	483	13.511425
21	565.56	0.9761	558	12.258261
22	621.11	1.0037	633	14.935056

23	676.67	1.0394	695	18.771590
24	732.22	1.0833	736	21.086734

First, the range of carbons in each cut was determined. If the TBP cut is treated as a multiple carbon number (MCN) group then the range of carbon compounds that satisfy equation 20 can be found[26].

$$M_I = M_n \left\{ \exp\left[(1/N_g) \cdot \ln(M_N / M_n) \right] \right\}^I \qquad \textbf{Eq. 20}$$

Equation 20 assumes that the molecular weights separating each MCN group can be described in terms of the first and the last component molecular weights of the range. Setting the number of MCN groups, N_g, equal the number of TBP cuts, where *I* is the number of the specific MCN group, an M_n and M_N, corresponding to the first and last component molecular weights respectively, can be found that satisfies the equation. Then matching that molecular weight to a particular single carbon number (SCN) compound the range of carbon compounds is found[27].

Once the range of carbon compounds was found that adequately represented the feed, the weight fraction of the individual compounds in that cut was found. In order to accurately determine the weight fraction of each component, the number of equations available to use must be equal to the number of components. This situation, however, was not the case. Therefore, an approximation was made[28].

Specific SCN components throughout the entire range of components were chosen to solve the equations available. Since accurate data was available for four different equations (21-24), four component weight fractions in each TBP cut range were initially found. After the weight fractions of these individual components were found their weight fractions were distributed uniformly over a number of compounds in the overall range[29].

$$\gamma_I = 1.0 / \left[\sum^{I} \left(f_{wi} / f_{wI} \right) / \gamma_i \right] \qquad \textbf{Eq. 21}$$

where γ = Specific gravity

f_w = Weight fraction

i = Single carbon number

I = Multiple carbon number

$$T_{bwI} = \sum^{I} (f_{wi} / f_{wI}) \cdot T_{bi} \quad \text{Eq. 22}$$

where T_b = Boiling point

$$p_{pcI} = \sum^{I} (z_i / z_I) \cdot p_{ci} \quad \text{Eq. 23}$$

where P_c = Critical pressure

z = Mole fraction

$$f_{wI} = \sum^{I} f_{wi} \quad \text{Eq. 24}$$

Once the weight fraction of each component was known the molar concentration is readily calculated based on the molecular weight, mass, and volume of the process stream. The volume used to calculate the molar concentration is the volume of the reactor.

MODEL VARIABLES AND LIMITATIONS

The main variables of visbreaking are temperature and residence time. In the model the temperature of the unit is specified, and the process is then considered isothermal. The range of possible input temperatures greater than actual range of temperatures for normal operation, thus the model can be used for both industrial designs. The mass flow rate is the other variable in the model. Through the mass flow rate the residence time of the process stream is determined. The residence time, however, is not accurately portrayed by the model. According to the model the reactions takes place at such a high rate that, for a temperature of 700K, the complete decomposition of the residue into gas happens within the first five feet of the reactor. Thus, it is important to note that the model only reflects one of the two major variables in visbreaking.

MODEL EQUATIONS

Equation 25 gives the difference of the component s_i's formation and its' cracking into lighter components. The first summation term, $\sum_{k=i+2}^{n} K_{k,i} Cs_k$, is what accounts for the formation of the s_i component, from i = s_i +2 to i = n, where n is the total number of i-carbon compounds. The summation is evaluated as follows: $K_{3,1}Cs_3 + K_{4,1}Cs_4 + K_{5,1}Cs_5 + K_{6,1}Cs_6 + K_{7,1}Cs_7 + \ldots + K_{n,1}Cs_n$ for $s_i = 1$. This accounts for each component greater than i+1 cracking into component i. Because a component can only break into components with less than i-1 it follows that s_i = n and s_i = n-1 will not have formation components.

$$rs_i = \frac{dCs_i}{dt} = \sum_{k=i+2}^{n} K_{k,i} Cs_k - Cs_i \sum_{j=1}^{i-2} K_{i,j} \qquad \textbf{Eq. 25}$$

The second term in the summation, $Cs_i \sum_{j=1}^{i-2} K_{i,j}$, accounts for the cracking of component i, for i greater than 2, into every component less than i-1. That is for n number of components, i = 3 to i

= n cracks into component i = 1 or $s_i = 1$. Because a component can only break into components with less than i-1 carbons it follows that $s_i = 1$ and $s_i = 2$ will not have cracking reactions. The summation is evaluated as follows: $Cs_n[K_{n,1} + K_{n,2} + K_{n,3} + K_{n,4} + K_{n,5} + \ldots + K_{n,n-2}]$ for $s_i = n$.

Equation 26 accounts for the o_i products of the cracking reaction. The summation starts at j = 3 for $o_i = 2$ and continues to j = n. That is that for every o_i, $i = o_i + 1$ to i = n cracks to form more o_i. However, since the terms in the summation are in the form of the components s_i the reaction constant is given as the constant for the reaction of component i cracking into $s_i = i - o_i$, where i changes from o_i - 1 to n and o_i is constant. The summation term is evaluated as follows: $K_{3,1}Cs_3 + K_{4,2}Cs_4 + K_{5,3}Cs_5 + K_{6,4}Cs_6 + K_{7,4}Cs_7 + \ldots + K_{n,n-2}Cs_n$ for $o_i = 2$.

$$ro_i = \frac{dCo_i}{dt} = \sum_{j=i+1}^{n} K_{j,j-i} Cs_j \qquad \textbf{Eq. 26}$$

The kinetic constant, $K_{i,j}$ (1/s), for the reactions is based on fitted parameters incorporating the molecular weights (PM) of i, and j; where i and j are the number of carbon atoms in the reactant and product, respectively. The molecular weights are determined as alkenes; that is 12*i +2*i. The reaction is assumed to take place isothermally to simplify the calculation of the rate constant.

$$K_{i,j} = A_{i,j} e^{-B_{i,j}/RT} \qquad \textbf{Eq. 27}$$

$$A_{i,j} = \left(a_0 + a_1 PM_i + a_2 \left[PM_i\right]^2\right) e^{-\frac{1}{2}\left(\frac{PM_j - \frac{PM_i}{a_4}}{a_3}\right)^2} \qquad \textbf{Eq. 28}$$

$$B_{i,j} = b_0 + b_1 PM_i + b_2 PM_j \qquad \textbf{Eq. 29}$$

Table 10: Constant used in $A_{i,j}$ and $B_{i,j}$

	A		B
a_0	1.51E+12	b_0	42894

a_1	**1.90E+08**	b_1	**-4.5**
a_2	**2.06E+06**	b_2	**3**
a_3	**146.95**		
a_4	**11.35**		

Equation 30 gives the rate of change of concentration for component s_i along the length of the reactor. The pipe diameter, ϕ, used in the calculation is the average of the pipe diameters used in the determination of the kinetic model: ϕ = 9.05 cm. The density, ρ, of the fluid was approximated as the average density of the feed according to the equation: $\overline{\rho} = \sum_{i=1}^{n} x_i \rho_i$, where x_i is the weight fraction corresponding to the density ρ_i. This equation results in a density of 0.998 g/cm^3. The rate of change reaction of s_i, rs_i, is given by equation 25 above in gmol/(cm^3-s). The flow rate, F, is given in g/s.

$$\frac{dCs_i}{dz} = \frac{1}{4}\pi\phi^2 \frac{\rho}{F} rs_i \qquad \textbf{Eq. 30}$$

Equation 30 is the same as equation 31 but it determines the change in concentration for component o_i along the length of the reactor[30].

$$\frac{dCo_i}{dz} = \frac{1}{4}\pi\phi^2 \frac{\rho}{F} ro_i \qquad \textbf{Eq. 31}$$

Equation 30 is used to find the change in Cs_i, dCs_i, for a given length increment dz in centimeters. The new Cs_i is then found from $Cs_i = Cs_i + dCs_i$, which is used in equation 25 to calculate rs_i. In this way equations 25-26 and equations 30-31 are integrated using the finite difference method. Equations 27-29 do not change for differences in concentration, therefore, for a constant temperature are only calculated once.

PRODUCT GROUPS

The products of the model are grouped into four different categories according to carbon number. The gas fraction contains all the components from i=1 to 4. The gasoline fraction contains all of the components from i=5 through 165^{o}C. The gas oil contains the components from 165 to 350^{o}C and the residue is all the components above 350^{o}C. Using the normal boiling points of the SCN components the gasoline fraction stops at i=10. The gas oil contains carbons from i=11 to i=21, with the residue containing everything from i=22 to i=45.

ISOMERIZATION

Isomerization is typically a gas-phased catalyzed reaction. It is an equilibrium reaction favored by lower temperatures. As the temperature of the unit increases the equilibrium shifts towards the straight chain molecules. The reaction occurs in a fixed bed, with recycling of the unreacted paraffins being a typical step in production.

PROCESS CHARACTERISTICS

Typical isomerization processes include a fixed catalyst bed reactor with separation and recycle equipment. The overall process varies according to the catalyst used. All processes require the input of hydrogen into the reaction although hydrogen is not consumed in any significant amounts. This hydrogen is typically recycled as is any paraffin that is not reacted. If the chlorinated platinum on alumina catalyst is used then the driers and scrubber for HCl removal are necessary process steps. However, with the platinum on zeolite catalysts these steps can be omitted[31].

Typically pentane and hexane are isomerized in one unit and butane in a separate unit. This is not always the case. It depends on the purpose of the unit as well as the amount to be processed. The optimal conditions for operation are not the same for butane and hexane, therefore if one unit is used to covert a mixed feed of butane through hexane then the maximum amount of either butane or hexane will not be achieved. The model supposes that the feed to the unit contains butane through hexane[32].

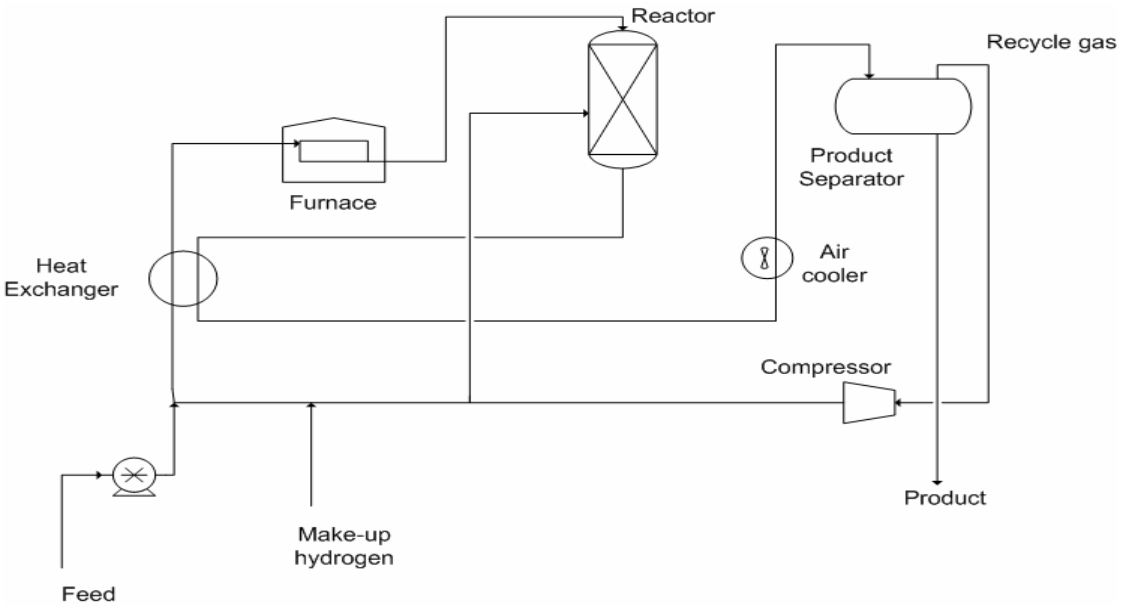

Figure 6: Typical Isomerization unit[33]

REACTION CHEMISTRY

Isomerization of n-alkanes is an equilibrium limited reaction. The equilibrium favors the isoparaffins at low temperatures; this is especially true for butane and pentane. However, this trend does not hold for all the isomers of hexane (Figure 7). 2,2-dimethylbutane (22-DMB) is the most stable and prevalent isomer of hexane at room temperature. Its presence decreases rapidly with increasing temperature. The other isomers of hexane, including n-hexane, all increase in mole percent as the temperature increases. The most prevalent at high temperatures, 250^{o}C, is 2-methylpentane (2-MP). The double branched carbon chains have the highest octane rating and are therefore the most desired. They are, however, due to the equilibrium described, typically not as stable at the operating conditions of most industrial processes. Also, due to the conditions of most industrial operations and the catalysts that are used, only one, 2-methylbutane, of the two pentane isomers forms, because of this, 2,2-dimethylpropane is not considered in the reaction process[34].

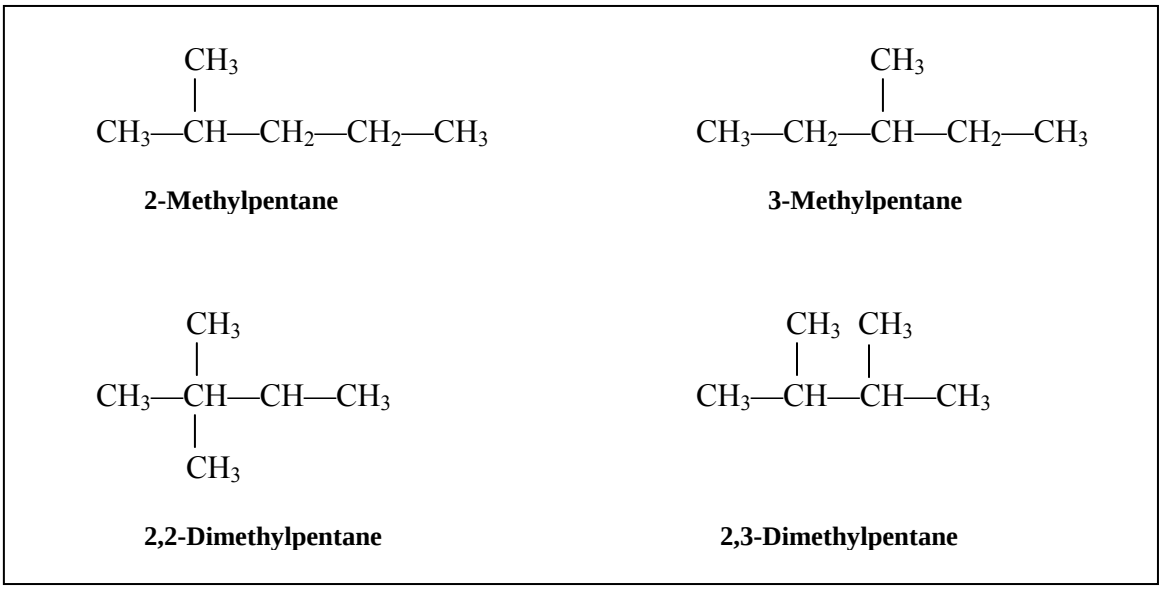

Figure 7: Isomers of Hexane[35]

The side reactions that accompany the isomerization process include cracking and coking. The amount of these reactions is typically dependent on the functionality of the catalyst used. However, if the hydrogenating function of the catalyst is greater than 15% of the acidic function then these side reactions are minimal[36]. In the model all side reactions are neglected.

CATALYSTS

Two types of catalysts, platinum/chlorinated alumina and platinum/zeolite, have become the most prevalent in industry. Both catalysts are bifunctional, with acidic and metallic sites, reacting by either a monofunctional or bifunctional mechanism. The operating conditions for each of these catalysts are given in table 11. The platinum/alumina catalysts operates at significantly lower temperatures, however, it requires that the feed is pretreated, particularly for water, and chlorine, usually in the form of carbon tetrachloride, must be continuously injected into the process stream. The injection of chlorine keeps the acidity of the catalyst at a maximum. One advantage of the platinum/zeolite catalyst is that it does not require that the feed be pretreated. However, the unit must operate at higher temperatures which reduces the amount of isomerate achievable with a single run[37].

As stated earlier, the side reactions for this unit can be minimized through the catalyst used. If the catalyst hydrogenating function to acid function ratio is above 0.15, then the catalyst activity, stability, and selectively are maximized and the side reactions are minimized[38].

Table 11: Operating conditions of catalyst used in industry[39]

	Pt on Chlorinated alumina	Pt on zeolite
Temperature (^oC)	**120-180**	**250-270**
Pressure (bar)	**20-30**	**15-30**
Space velocity (h^{-1})	**1-2**	**1-2**
H_2/HC (mol/mol)	**0.1-2**	**2-4**

FEED CHARACTERIZATION

Typical feeds for isomerization units are either from straight-run crude distillation or catalytic reforming. Feeds usually contain roughly 50wt% pentanes and 50wt% hexanes. The feed for butane process is roughly the same as that for pentane/hexane process. The butane fraction will range from 0 to approximately 3wt%[40]. Using these weight fractions, the number of moles and mole fractions are easily calculated using the molecular weights of each component. However, the rates described above require the components to be in the form of partial pressure and molar concentration.

Using Antoine's equation and Wagner's equation to determine the vapor pressures of each of the components at the unit temperature, the components partial pressure can be found from using the mole fraction determined above[41]. The sum of the individual partial pressures gives the total pressure of the unit. The desired hydrogen to hydrocarbon ratio of 0.5 to 2 gives the pressure of hydrogen supplied to the reaction. An approximation of the process stream volume and the

concentration of hydrogen can then be found with the ideal gas law. These calculations give the feed in all the forms needed for the rate law calculations.

MODEL VARIABLES AND LIMITATIONS

The model has three inputs: temperature, mass flow rate, and hydrogen to hydrocarbon ratio. The mass flow rate has no limitation its' value. The H_2/HC ratio limitation is set by normal practice between 0.1 to 2. The temperature, however, does have limitations in the model that are not present in normal industry. Depending on the catalyst the temperature of an isomerization unit can range from 120 to 270^{o}C. Using the Wagner equation to calculate the vapor pressure sets the upper limit on the unit temperature at 187^{o}C due the use of critical temperature. Above the critical temperature the Wagner equation fails. However, the 187^{o}C covers the range of operating temperatures for the Pt/alumina catalyst which was used to develop to of the rate equations.

N-BUTANE MODEL[42*]

The isomerization of n-butane can be model based on the partial pressure of n-butane and hydrogen according to the rate law:

$$r_{n-C4} = -K_1 \cdot \frac{P_{n-C_4}}{P_{H_2}} + K_2 \cdot \frac{P_{iso-C_4}}{P_{H_2}} \qquad \textbf{Eq. 32}$$

where K_1 and K_2 (atm/s) are the rate constants for the forward and reverse reactions respectively. This rate law was determined using NIP-66 catalyst. This catalyst contains 0.6% Pt and 6-10% Cl on n-Al_2O_3[43].

Table 12: Activation Energy and Frequency Factor for n-Butane Isomerization

	E, J/mole	A
K_1	**58,615**	**3,953,058**
K_2	**66,989**	**25,140,735**

N-PENTANE MODEL[44*]

Due to the selective of the catalysts used in industry one of the isomers of the n-pentane, 2,2-dimethylpropane, does not form in an appreciable amount and thus can be disregarded when considering the isomerization reaction[45]. The reaction of n-pentane to isopentane or 2-methylbutane can be based on a general first order rate law. Based on molar concentration, a rate law can be developed that takes into account the effective rate of reaction accounting for the actual rates variation with both hydrogen and hydrocarbon content. The equation

$$R \ln K_{eq} = \frac{1861}{T} - 1.299 \qquad \textbf{Eq. 33}$$

allows calculation of the equilibrium constant for variations in temperature. Using the equilibrium constant, a rate equation (33) based on the molar concentration of n-pentane, isopentane, and hydrogen can be used to predict the product of the isomerization reaction. This rate is also determined on the NIP-66 catalyst.

$$r_{n-C5} = -\left[K_2 \cdot \left(\frac{C_{n-C5}}{[H_2]} \right)^{0.125} - 0.0000197 \cdot t \right] \left[K_{eq} \cdot C_{n-C5} - \left(K_{eq} + 1 \right) \cdot C_{i-C5} \right] \qquad \textbf{Eq. 34}$$

Table 13: Activation Energy and Frequency Factor for n-Pentane Isomerization

	E, J/mole	A
K_1	42,287	4,024
K_2	50,032	7,332

* The majority of the each of the sections is taken from the reference given with the section heading.

N-HEXANE MODEL[46*]

n-Hexane has four different isomers that it can form as shown in Figure 7. Each of the five total compounds reacts to form the other four as in Figure 8. All of these reactions must be taken into account in the model. For a constant pressure, all of these reactions can be consider by a first order rate law. Thus, the general rate equation (35) can be used to predict the products of the isomerization reaction. Equation 35 uses molar concentrations of the components. The rate was developed using a Pt-H-for mordenite (Pt/HM) catalyst.

$$\frac{dC_i}{dt} = -\left(\sum_{j=1}^{5} K_{j,i}\right)\cdot C_i + \sum_{j=1}^{5} K_{i,j} C_j \qquad \textbf{Eq. 35}$$

Table 14: Nomenclature used in the reaction rate equation for n-Hexane

n-Hexane	**1**
3-MP	**2**
2-MP	**3**
2,3-DMB	**4**
2,2-DMB	**5**

Where the rate constants are evaluated, using the nomenclature in table 14, as $K_{1,2}$ being the rate constant for the reaction of 3-MP to n-Hexane. The rates of each of the reactions in figure 8 were found for three different temperatures. Rearranging the Arrhenius equation to the form of

$$\ln(K) = \ln(A) - \left(\frac{E}{R}\right)\left(\frac{1}{T}\right) \qquad \textbf{Eq. 36}$$

the activation energies and the pre-exponential factors for the reactions were found and are presented in tables 15-16. With these values and equation 35 the products of the isomerization reaction of n-hexane can be predicted.

Table 15: Activation Energy and Frequency Factor for n-Hexane Isomerization

	n-C6		3MP		2MP	
	-E/R	A	-E/R	A	-E/R	A
n-C6	0	0	-19406	1.25E+16	-19666	2.57E+16
3MP	-23035	1.12E+19	0	0	-15184	4.7E+13
2MP	-20758	7.68E+16	-16076	1.68E+14	0	0
23DMB	-23784	1.97E+18	-21259	2.66E+17	-19478	5.56E+16
22DMB	-14552	7.10E+09	-27669	4.48E+21	-9480	1.97E+06

Table 16: Activation Energy and Frequency Factor for n-Hexane Isomerization

	23DMB		22DMB	
	-E/R	A	-E/R	A
n-C6	-29556	1.2E+24	-25756	9.3E+19
3MP	-15982	1.61E+13	-26796	3.53E+21
2MP	-16134	2.8E+13	-25562	3.02E+20
23DMB	0	0	-16446	2.00E+13
22DMB	-18192	2.98E+14	0	0

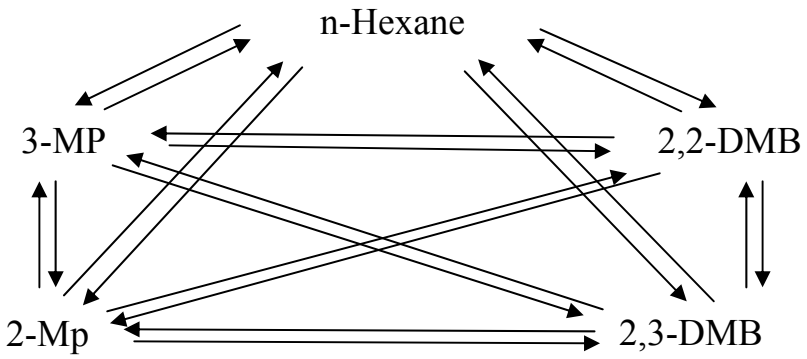

Figure 8: Reaction Pathways for n-Hexane and its isomers[47]

PRODUCTS

Using finite integration the rates equations can be solved for incremental time periods. The products of both n-hexane and n-pentane with their respective isomers are in the form of molar concentrations. These concentrations can easily be converted back into the weight percents using the volume calculated for the feed and the molecular weight of each component. The n-butane and isobutane products, however, are in the form of partial pressures. Assuming the reaction to occur at constant pressure, these partial pressures when put as a ratio over the total pressure yield

the mole fraction of both isobutane and n-butane. Since the total number of moles of n-butane and isobutene do not change in an isomerization reaction, using the product mole fraction the distribution of the moles of each of the components can be found according to the equation:

$$\frac{\text{mole fraction isobutane}}{\text{isobutane fraction} + \text{n} - \text{butane fraction}} \times \text{moles of feed n} - \text{butane} \qquad \textbf{Eq. 37}$$

Once the number of moles is found the weight fraction is readily calculated.

HYDROCRACKING

INTRODUCTION

Hydrocracking is a process in which petroleum feed stock is reacted over zeolite catalyst with hydrogen to reduce the size of species in the feed[48]. Feedstocks for hydrocrackers include heavy distillate stocks, aromatics, cycle oils, and coker oils. Large molecules found in feedstocks can be broken down by this process yielding more valuable light products that can be readily used as fuels. Hundreds of reactions take place in a hydrocracker. Of these, many fall under the categories of catalytic cracking coupled with hydrogenation of hydrocarbons, hydrogenation of condensed aromatic compounds, and isomerization. The main two reactions, cracking and hydrogenation, are complementary in that the cracking reactions provide olefins for hydrogenation while the hydrogenation reactions provide heat for cracking. These reactions are summarized below.

Cracking reactions	Hydrogenation reactions
R-C-C-C-R + heat → R-C=C + C-R	R-C=C + H_2→ R-C-C + heat

Other reactions of the process are the reduction of nitrogen compounds and sulfur into ammonia and hydrogen sulfide. Typically the amount of sulfur and nitrogen compounds in the feed are kept rather low because these reactions can foul the catalyst. These side reactions do however clean the products and help maintain environmental regulations.

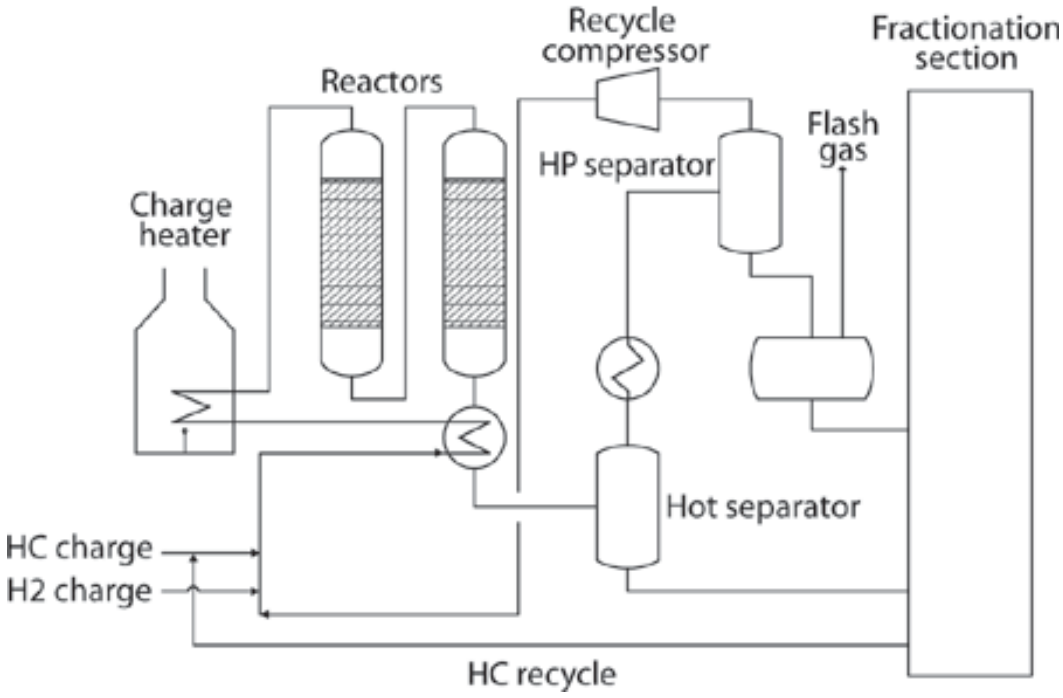

Figure 9: Hydrocracking PFD[49]

Typical operating conditions are summarized in the following table[50]. The range for distillate hydrocracking is wide that that of residuum cracking since the properties of distillates can vary greatly.

Table 17: Typical Hydrocracking Operating Conditions

	Residuum	Distillate
Hydrogen Consumption (SCFB)	1200-1600	1000-2400
LHSV (hr^{-1})	0.2-1	0.5-10
Temperature (°F)	750 -800	500-900
Pressure (psi)	2000-3000	500-3000

PURPOSE

The purpose of this model is to predict yields of the hydrocracking process based on characterized feed inputs.

MODEL

This model is based on data obtained from Nelson[51] who derived some simple graphs and correlations from experimental data to estimate hydrocracking yields.

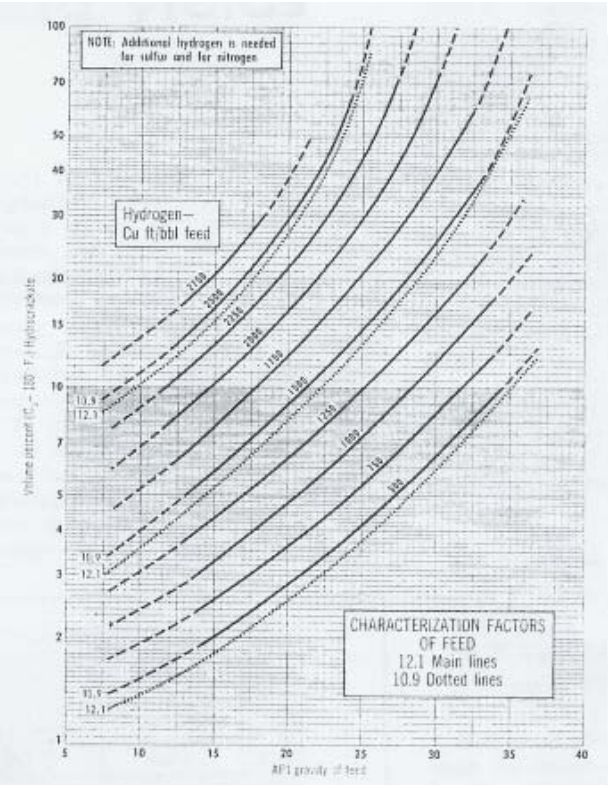

Figure 10: Yield of Light Naphtha[52]

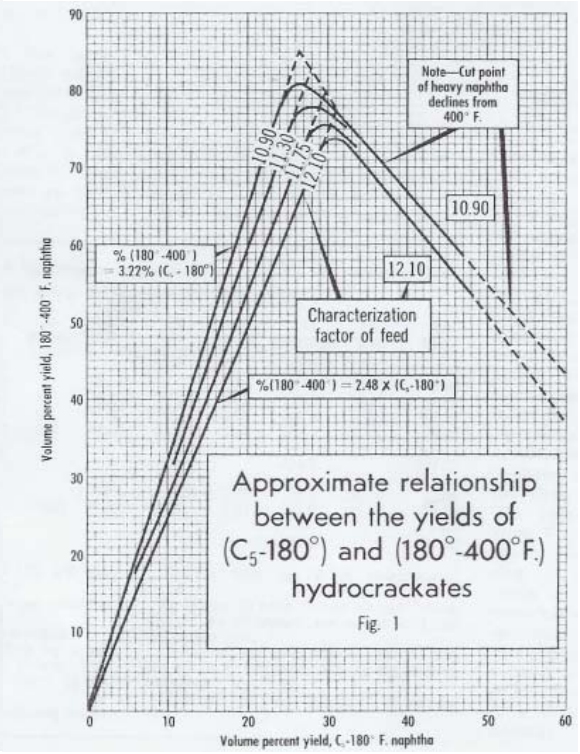

Figure 11: Yield of Heavy Naphtha[53]

The aim of this model is to make these graphs continuous for entire range of input variables, fit the graphical data, and consolidate these equations into a single input/output relationship.

Nelson constructed a graph that would predict the volume percent of light naphtha, p_1, based on three variables: the amount of hydrogen consumed, the Watson characterization factor of the feed, and °API (API gravity) of the feed. First the relationship of volume percent of light naphtha vs. Hydrogen feed rate (SCFB) of the feed was determined by taking the K_w=12.1 curves and fitting them with exponential equations of the form,

$$vol\% p_1 = Ae^{B \bullet H} \qquad \textbf{Eq. 38}$$

where H is the hydrogen Feed rate (Standard cubic feet per barrel of feed) and the coefficients A and B were determined for each °API curve.

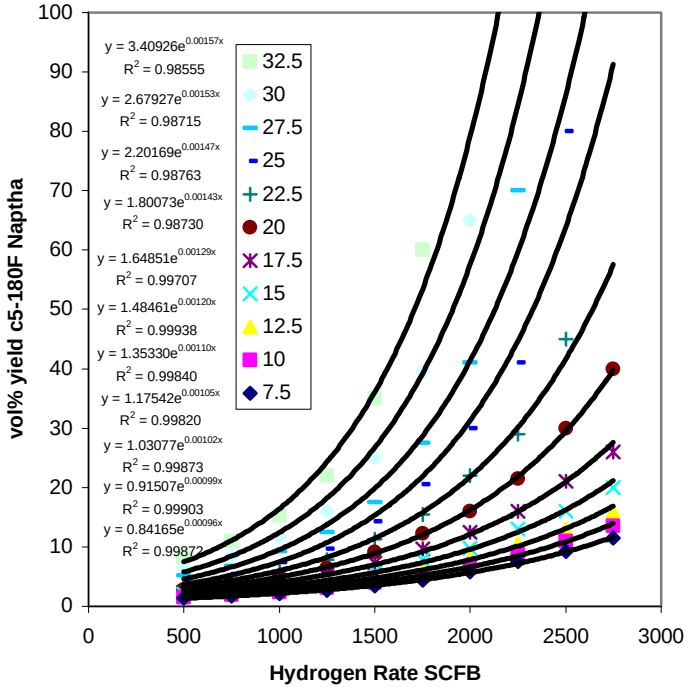

Figure 12: Yield of Light Naptha vs. Hydrogen Feed Rate

These coefficients were then fit with polynomial equations so that a continuous set of curves could be determine for any given hydrogen flow rate and °A PI of the feed.

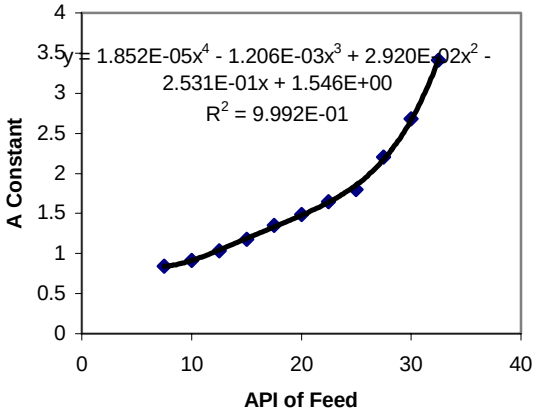

Figure 13: Coefficient A vs °API of Feed

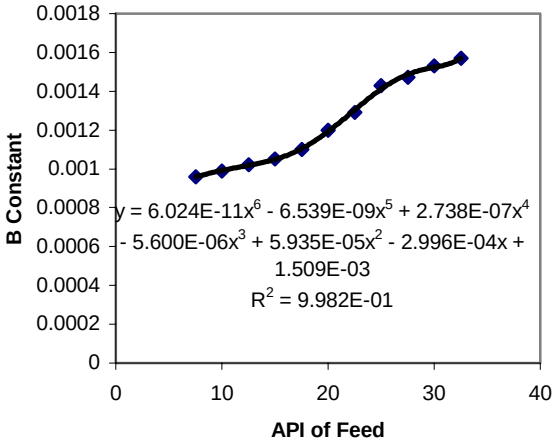

Figure 14: Coefficient B vs. °API of the feed

The polynomials are as follows:

$$A = 0.00001852(°\text{API})^4 - 0.001206(°\text{API})^3 + 0.0292(°\text{API})^2 - 0.2531(°\text{API}) + 1.546$$

$$B = 6.024\text{E}-11(°\text{API})^6 - 6.539\text{E}-09(°\text{API})^5 + 2.738\text{E}-07(°\text{API})^4 - 5.600\text{E}-06(°\text{API})^3 + 5.935\text{E}-05(°\text{API})^2 - 2.996\text{E}-04(°\text{API}) + 1.509\text{E}-03$$

Eq. 39

The second relationship that was developed was the affect that K_w had on the yield. Since there were only two different K_w values plotted on the graph, a simple analysis was conducted. By comparing the curves of different K_w values that had the same hydrogen feed rate, it was determine that there was about a 10% greater yield for the lesser K_w value for any given hydrogen feed rate.

Table 18: Effect of K_w on yield of Light Naphtha

		°API							
Hydrogen Rate(SCFB)		7.5	10	12.5	15	17.5	20	22.5	25
2500	K_w=12.1	9.25	11	13	16	21	30	45	80
diff. from	K_w=10.9	0.75	1	1	1.25	1.75	2.5	5	7.5
%diff.		8.11%	9.09%	7.69%	7.81%	8.33%	8.33%	11.11%	9.38%
1500	K_w=12.1	3.4	4	4.8	5.8	7.3	9.1	11.25	14.25
diff. from	K_w=10.9	0.35	0.45	0.5	0.55	0.7	1	1.5	1.75
%diff.		10.29%	11.25%	10.42%	9.48%	9.59%	10.99%	13.33%	12.28%
500	K_w=12.1	1.4	1.55	1.7	2	2.3	2.8	3.4	4.2
diff. from	K_w=10.9	0.1	0.17	0.2	0.2	0.25	0.3	0.35	0.4
%diff.		7.14%	10.97%	11.76%	10.00%	10.87%	10.71%	10.29%	9.52%

Thus the relationship of yield versus K_w was assumed to be directly proportional. That is, a change in K_w of 1.2 would yield a change in yield of 10 percent. With this correction factor the light naphtha yield equation now becomes

$$vol\% p_1 = (1.00833K_w - 0.00833)Ae^{B \bullet H} \qquad \textbf{Eq. 40}$$

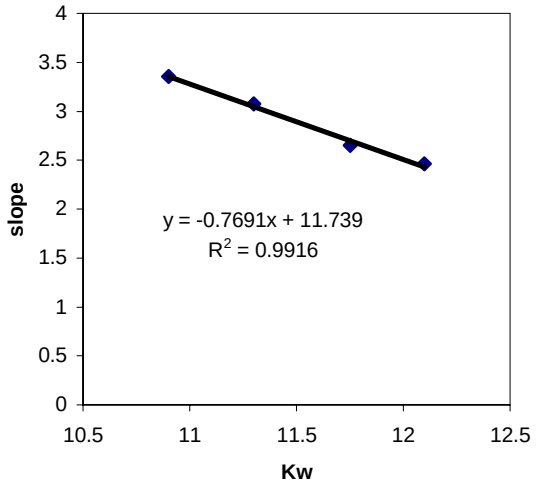

Figure 15: Slope of Heavy Naphtha Yield Relationship

This second product that was obtained was heavy naphtha, p_2. Nelson used correlated data to obtain a graph of vol% p_1 vs vol% p_2 with K_w of the feed as a parameter. This graph was made continuous over all values of K_w so that the model would determine the yield of heavy naphtha over the entire range of K_w. K_w was determined to linearly affect the relationship of p_1 and p_2. It

should be noted that this graph also showed that at some point the heavy naphtha would start to break down into light naphtha. It was assumed that this would not be desirable for operation of this unit and this portion of the graph was not considered in the model. That is, you would not want to operate at these conditions so you would not consider these outputs. Outputs of p_1 that would give these conditions are at the limit of correlations used to obtain p_1. The yield of p_2 that was developed is as follows

$$vol\%p_2 = (-0.7691 \cdot K_w + 11.739)(vol\%p_1) \quad \textbf{Eq. 41}$$

The third, fourth, and fifth products, iso-butane, n-butane, and C3+ lighter respectively, were determined by Nelson by correlating 170 sets of data from literature. These amounts can be found with the following relationships:

$$vol\%p_3 = 0.337(vol\%p_1) \quad \textbf{Eq. 42}$$

$$vol\%p_4 = 0.186(vol\%p_1) \quad \textbf{Eq. 43}$$

$$vol\%p_5 = 1 + 0.09(vol\%p_1) \quad \textbf{Eq. 44}$$

Using the volume percents of the products the weight percents were able to be determined by a relationship that was developed by Katz and Firoozabadi[54]. A correlation was developed by fitting data of density vs. average boiling point. Data was obtained for the chosen for the range needed, and a best fit equation was developed. The results are shown below.

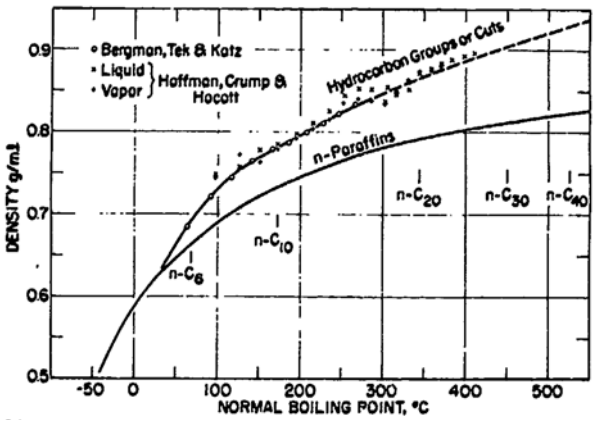

Figure 16: Density vs. Average Boiling Point[55]

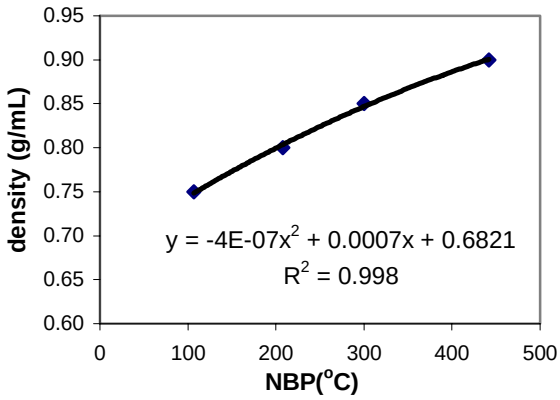

Figure 17: Density vs. Average Boiling Point

These five equations were put into a spreadsheet so that the inputs and outputs could be connected to other refinery streams. Error associated with this model was evaluated by comparing values read off of the graphs and those that the model produced. Results and the associated error are summarized in the following table.

Table 19: Error Associated with the Model

°API	Hydrogen (SCFB)	K_w	vol% p_1		vol% p_2	
15	2500	12.1	16.4	9%	39.9	1%
actual			15.0		40.5	
20	750	10.9	3.3	7%	11.0	9%
actual			3.5		10.0	
30	1250	10.9	16.3	25%	54.7	27%
actual			13.0		43.0	

At high feed °API the error becomes large due to the exponential increase in yield and the shortcoming of the model's fit of this relationship.

POSSIBLE MODIFICATIONS

Modifications to this model would include calculating the amount of additional hydrogen that would be consumed in the reduction of the nitrogen and sulfur compounds and that which would be lost do to saturation of the products. An economical analysis of the energy requirements and operating cost should be done so as to optimize the overall refinery model.

POSSIBLE ALTERNATIVE MODELS

Other models that were found in literature that could be used to determine hydrocracker yields include ones developed by Strangeland[56] and Laxminarasimhan et al.[57] Strangeland developed a kinetic model for the prediction of hydrocracker yields. The model has only inputs of pseudo components of the feed and time. There also three parameters, A, B, and C, in the model that allow for flexibility of the model to be applied to many different units.

Another alternative to the presented model is a continuous lumping model for hydrocracking developed by Laxminarasimhan et al. Inputs of this model are the true boiling point curve of the feed and time. This model contains five tuning parameters. This model used an integrative approach to determine the distribution of products as a continuous true boiling point curve.

SOLVENT DEWAXING

INTRODUCTION

Solvent dewaxing is a process in which high pour point waxes are separated from lubricating feedstocks.[58] Typical feedstocks include distillate and residual stocks with heavy gas oils being the primary feed. The lubricating oil pour point depends primary on the amount and size of n-paraffins present. Solvent dewaxing involves the use of solvent addition and refrigeration to crystallize the n-paraffins in the feedstock. The paraffin wax crystals can then be separated out of mixture by filtration. The solvent is used to decrease the viscosity of the feed to allow for ease of pumping and filtering. Common solvents include several different ketones and also propane. After wax separation the filtrate, or dewaxed oil, is then sent to an evaporator to remove the more volatile solvent. The oil also undergoes steam stripping to remove any traces of solvent. Typical operating conditions include solvent to oil ratios of 1:1 to 4:1 and also the desired pour point temperature of product. The product pour point is the operating temperature of the chiller or slightly lower. The wax filter cake then undergoes several steps to remove the solvent and any remaining oil that is trapped in the crystal structure. These steps include solvent washing, evaporation of the solvent, and steam stripping to remove any traces of solvent.

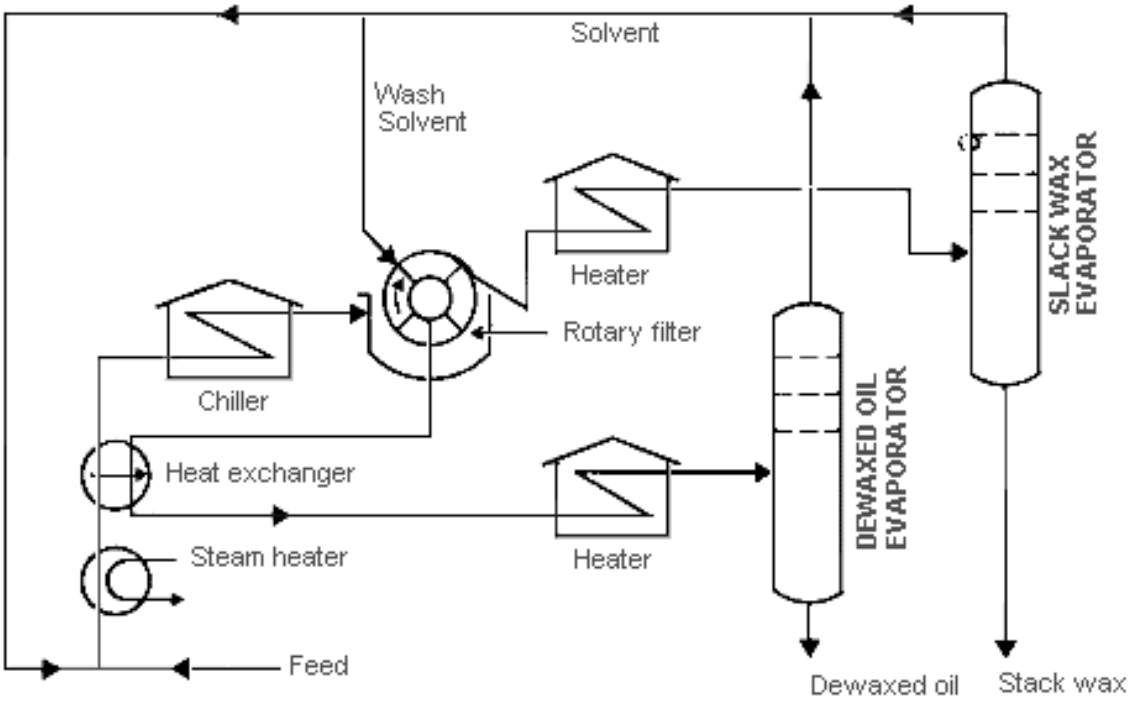

Figure 18: Solvent Dewaxing PFD

PURPOSE

The purpose of this model is to predict yields of a solvent dewaxing process based on characterized feed inputs.

MODEL

This model is based on correlated data from Krishna.[59] Krishna developed a correlation between PC (wt %), the percent of C_{15}+ n-paraffins, with the average chain length, CL, of these paraffins, and the pour point of gas oils.

$$PPT = A0\log\left(100/PC\right) + \left(A1/CL\right) + A2 \qquad \textbf{Eq. 45}$$

The three compositional parameters, A0, A1, and A2, need to be experimentally determined for each feed. By removing or adding incremental amounts of wax in the oil feed and measuring the pour point of each sample these parameters can be determined experimentally with linear regression of the data.

Once these parameters are known, the pour point of the feed can be determined. For a given desired product pour point , the maximum allowable wax content in the product can be determined by solving the equation for PC.

$$PC = \frac{100}{10^{\left[\frac{PPT+\left(A1/CL\right)+A2}{A0}\right]}} \qquad \textbf{Eq. 46}$$

Using a mass balance the yield of dewaxed oil is determined.

$$OilYield(wt\%) = \frac{\left(100 - PC(feed)\right)}{\left(100 - PC(product)\right)} \qquad \textbf{Eq. 47}$$

Since the separation is just filtering solids out of slurry, the theoretical yield is a good estimate of the actual yield. An analysis was conducted to see how the error associated with the correlation would propagate through the mass balance model. Given the data from Krishna,[60] a percent error was determined for predicted pour point of the feed. This error was then applied to the desired pour point to determine a range of allowable wax percent in the product. The error is the percent difference of the yield for the low and high yield.

Table 20: Error Analysis of Correlation

	BC2	NC6	NC7	NC8	NC9	NC10
°C	375-500	375-400	400-425	425-450	450-475	475-500
wax wt%	46.8	44.88	47.28	48.41	48.72	47.05
CL	26.89	24.13	25.13	27.14	29.05	31
PPT act.	48	39	45	48	51	57
PPT pred.	48.0	41.0	44.0	48.9	52.8	55.9
error %	0.1%	5.0%	2.3%	1.8%	3.5%	1.9%
dewaxing model		Desired PPT=	10			
PPT low	9.99	9.50	9.77	9.82	9.65	9.81
PPT high	10.01	10.50	10.23	10.18	10.35	10.19
wax wt% low	0.368	0.819	0.608	0.336	0.202	0.133
wax wt% high	0.369	0.931	0.643	0.352	0.220	0.139
yield low	0.5340	0.5558	0.5304	0.5176	0.5138	0.5302
yield high	0.5340	0.5564	0.5306	0.5177	0.5139	0.5302
error %	0.001%	0.112%	0.036%	0.016%	0.019%	0.006%

POSSIBLE MODIFICATIONS

An economical analysis of the utility costs (including refrigeration, electricity, etc.) should be done so as to optimize the overall refinery model. Relationships should also be obtained to link properties of the feed to the compositional parameters.

POSSIBLE ALTERNATIVE MODELS

A thermodynamic model using pseudo components could be constructed by using the average crystallization point of each component and the average molecular weight. These values could be obtained from the correlations found in literature[61],[62]. For an accurate model of this type, the amount and distribution of molecular weights of paraffin wax would need to be known about the feed. These characteristics would most likely have to be obtained analytically.

ALKYLATION

PURPOSE

Alkylation is a process similar to polymerization in the respect that both combine short chain gases into long chain saturated liquid hydrocarbons. Typically the reaction combines isobutene with a propylene/butylene mixture by means of an acid catalysis. Alkylation processes vary greatly from refinery to refinery, since individual technology is usually patented. Therefore, the following process flow diagram is a specific design patented by Exxon-Mobil.

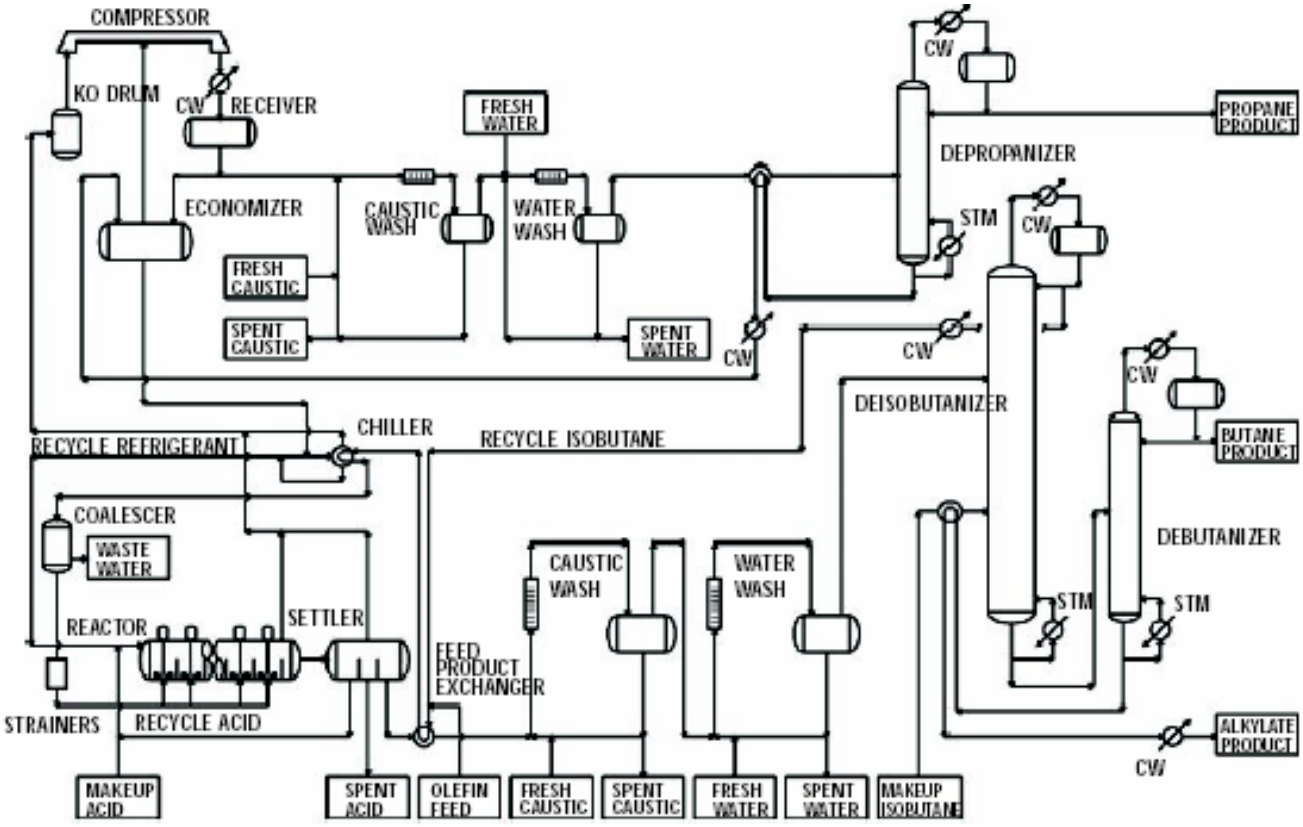

Figure 19: Exxon-Mobil Auto refrigeration H2SO4 alkylation[63]

INTRODUCTION

Alkylation has been around since the 1930s. The product of alkylation, alkylate, is highly valuable because of its extremely high octane number. During WWII, alkylate production increased dramatically because of ability to increase the performance of piston driven aircraft dramatically. After WWII and the advent of the jet engine alkylate production dropped dramatically. However, alkylation within the last thirty years has seen a rapid expansion, due to the need for high octane, low emission fuels. Typically alkylation units consist of a CSTR fed a hydrocarbon mixture of liquefied isobutene/butylene/propylene and an equal feed of a strong aqueous acid. Of which the commercial alkylation units within the past decade using sulfuric acid (H_2SO_4) or hydrofluoric acid (HF) are the most popular, with 70% of new units being H_2SO_4. The reason for the popularity of H_2SO_4 over HF is related to the nature of handling HF, and due to the fact that HF catalysis consumes more isobutene. [64]Therefore, H_2SO_4 catalysis will be considered.

Essentially alkylation can be described as a series of reaction happening simultaneously, with different reaction rates competing with each other. Different side reactions include[65]:

- Polymerization (e.g. $2C_3H_6 = C_6H_{12}$)
- Hydrogen Transfer (e.g. $2i\text{-}C_4H_{10} + C_6H_{12} = C_8H_{18} + C_6H_{14}$)
- Disproportionation (e.g. $2C_8H_{18} = C_7H_{16} + C_9H_{20}$)
- Cracking (e.g. $C_{12}H_{26} = C_7H_{14} + C_5H_{12}$)
- Esterification (e.g. $2C_4H_{10} + H_2SO_4$ = di-butyl sulfate, decomposes in downstream equipment causing corrosion)

In order to maximize the final product and produce alkylate economically operating tolerances are small. The primary cost associated with alkylation is acid degradation, which is addressed in several different ways. In HF alkylation units regenerating HF can be done in house while H_2SO_4 has to usually be sent to a separate facility. Therefore, in order to maintain 95% H_2SO_4 in the reactor, new acid needs to be added constantly. This is because the most desirable C_8 structure, trimethypentanes (TMPs) with research octane numbers (RONs) of 100-109.6 [66] are easily oxidized. "During the oxidation, SO_2 and water are produced as the sulfuric acid reacts"[67] which in effect reduces the quality of the product and acid catalysis. This example highlights another complexity of the alkylation process, not all C_n structures have octane numbers corresponding to the number of carbon. For example, dimethylhexanes are C_8 structures with RONs in the 55.5-76.3 range, while dimethylpentanes, a C_7 structure, have are usually 89-91.[68] To further complicate the issue, dimethylhexanes with a span of 20.8, estimating an octane number from a mixture of propylene, butylenes and isobutane is all but impossible even if the exact distribution is known.

Since the exact octane of the final product would depend on exactly what structures are present in the final product (ie 2,2,4-TMP has a different octane rating than 2,4,4-TMO) and there is no kinetics to describe this branching, kinetic modeling is useless. To model alkylation purely by mechanism kinetics would be ludicrous, and would not give a suitable prediction of the final product. In 1972, Langley et al. developed a kinetic model for alkylation of isobutene with pure propylene. In their paper they explained "the kinetics of the reaction have remained largely

unexplored."[69]Nevertheless, they attempt to model the reaction in which the products, as they describe them, are structures based purely on the number of carbons present. As stated previously trying to describe an octane rating based on number of carbon present is like predicting the horsepower of a car by its color- grossly inaccurate. To further add to the problems of their model, they only consider a feed of pure propylene with isobutene. In fact most alkylation processes use a mixture of mixed-butylenes, propylene, and isobutene for which all three will interact with each other.

As of 2003, "For alkylation in a cascade reactor using sulfuric acid as the catalyst, 32 events (or steps) have been identified."[70]Although these steps have been identified, quantifying them into useable data is difficult or impossible due to the nature of them. For example, the dispersion of droplets in the two phase acid/hydrocarbon phases and the subsequent transfer between the interfaces are difficult to quantify because they depend on, temperature, flow pattern, size and shape of the droplets, and the specific hydrocarbon being transferred.[71] This step, along with others has been described as specific, to the particular apparatus being used. In fact in 1995 a team at Purdue University explained "Information on the interfacial areas of in the reactors is needed to explain the overall mechanism and kinetics of alkylation since both chemical and physical phenomena have a major effect on the reactions. Unfortunately, such information is not yet available."[72] Therefore the kinetics of alkylation is impossible, and correlation factors must be used.

MODEL

The model used to describe the alkylation process was based on that A.V. Mrstik et al.[73] He assumes that since most alkylation systems use large cooling systems implement a system where the reacting products drive the cooler that temperature is constant, between 40° and 50° F. Therefore the correlation factor breaks down to be:

$$F = \frac{I_E (I/O)_F}{100(SV)_O} \qquad \textbf{Eq. 48}$$

Where

$(I/O)_F$ = volumetric isobutene-olefin ratio in reaction feed

I_E = liquid volume percent isobutene in reaction effluent

$(SV)_O$ = olefin space velocity in volumes per hour per reactor volume

F= Factor designed by A.V. Mrstik et al.

It follows that by calculating this factor it can be correlated to the following graph, depending on the starting material.[74]

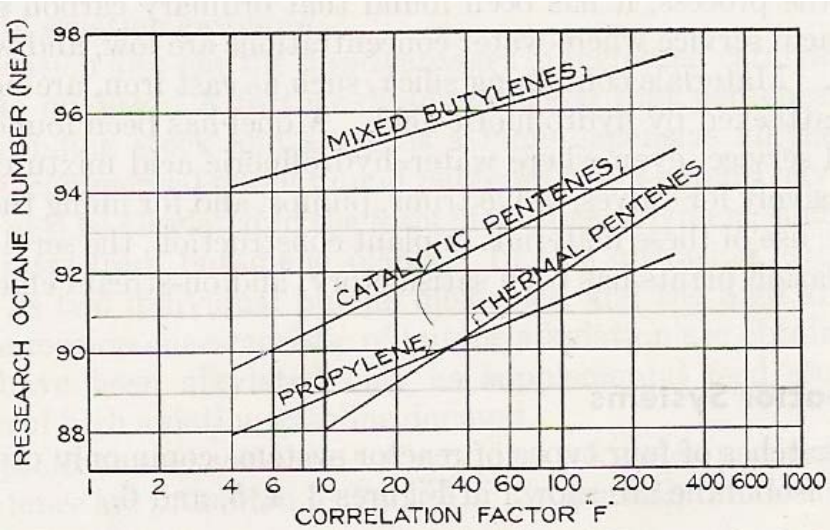

Figure 20: Sulfuric Acid Alkylation relating "F" factor to octane number [75]

As for acid consumption, it was correlated by a linear relationship, described by D.H. Putney, between octane number and acid consumption.[76] Typically acid consumption is related to the efficiency of the process, because TMP contribute to the high octane, yet are consumed by dodgy systems.

POSSIBLE MODIFICATIONS

In order to improve this model, more factors should be considered. For example, amount of mixing needs to be added to the "F" correlation factor. This could be in the form of horsepower input per barrel fluid that relates to a completion factor. Also rather than considering all inputs as

individuals, a correlation could be used to account for their interactions. Describing the overall process is difficult at best. In an actual before a refinery builds an alkylation process, they know the optimal operating conditions. Therefore and changes from the set point is considered deviations and they are corrected. Essentially, alkylation is not a new process; therefore every combination of every variable at some point in the last 80 years has been tried. Developing a theoretical model that improves the reaction just a small amount will most likely be within the error of the model. Hence any conclusion that is reached cannot be confirmed without experimental results. Alkylation is such a difficult process to model, and is dependent on so many variables that many companies forgo designing their own and buy the rights from another company.

POLYMERIZATION

PURPOSE

Polymerization in principle is very similar to alkylation. Both processes combine light gases like isobutene, butylenes, and propylene into higher chain length hydrocarbons that can be used for gasoline or diesel mixtures.

INTRODUCTION

Catalytic polymerization when it was first introduced in the 1930s typically used a solid phosphoric acid (SPA) catalysis that converted propylene into saturated alkanes of varying length. The primary problems with polymerization were that the incoming streams had to be rid of oxygen and sulfur in order to prevent catalysis poisoning. In addition controlling the distribution of chain lengths was difficult. Therefore the process fell out of popularity in the 1960s.[77]

In its second life, polymerization of propylene and butylenes using zeolites has gained attention. Several companies including Exxon-Mobile have issued patents for these processes with different zeolites (ZSM-5 and ZSM-12) with the hope that with one unit both high cetane diesel and high octane gasoline can be produced.[78]

The octane number is of course the unit of measurement for the ability of a gasoline to be compressed without premature ignition. A higher octane number usually corresponds to a higher allowable compressibility. Hypothetically, pure isooctane has an octane rating of 100. Different standard of measuring octane have been introduced over the years. Meanwhile, the cetane (hexadecane, $C_{16}H_{34}$) number is the diesel equivalent, measuring the combustibility of diesel.

The process being followed is the MOGD (Mobile olefin to gasoline and distillate) process described by S.A Tabak et al.[79] For this process propylene and butylene are passed through ZSM-5 and emerge a distribution of structures. The zeolite is used because the protonic acid that is located inside the zeolite functions as a catalyst, while the pore size controls the shape and size of the molecule.

MODEL

The model for zeolite polymerization is based on experimental data developed by the Mobil Research and Development Corporation.[80] In their experimentation they assumed that the purpose of this research is to develop a process that will be useful commercially. Therefore they assumed that the primary reactions of interest are those that have virtually 100% conversion. The three primary variables of temperature, pressure, and space velocity, are all interactive, and therefore all effect octane/cetane rating. To add to the complexity of the reaction, the temperature of the reactor can be difficult to maintain due to the nature of the high exothermic reaction (~1,550 kJ/kg propylene, depending on the chain length being produced). Therefore, liquid propane is usually required to be injected into the packed bed reactor to cool the mixture. Typically the charge going to the reactor is as followed.

Table 21: Typical charge

Propylene	12.0 wt%
Propane	10.7 wt %
1-butene	36.1 wt %
Isobutane	27.2 wt %

As for the temperature of the reactor, it is held at 550K through liquid propane injecting and steam generation. In order to change the average molecular weight of the product stream, and

thus the use (gasoline, diesel, or fuel oil) the partial pressure of the system is usually adjusted by means of an inert gas such as nitrogen. Changing the partial pressure has the following effect on average carbon length.

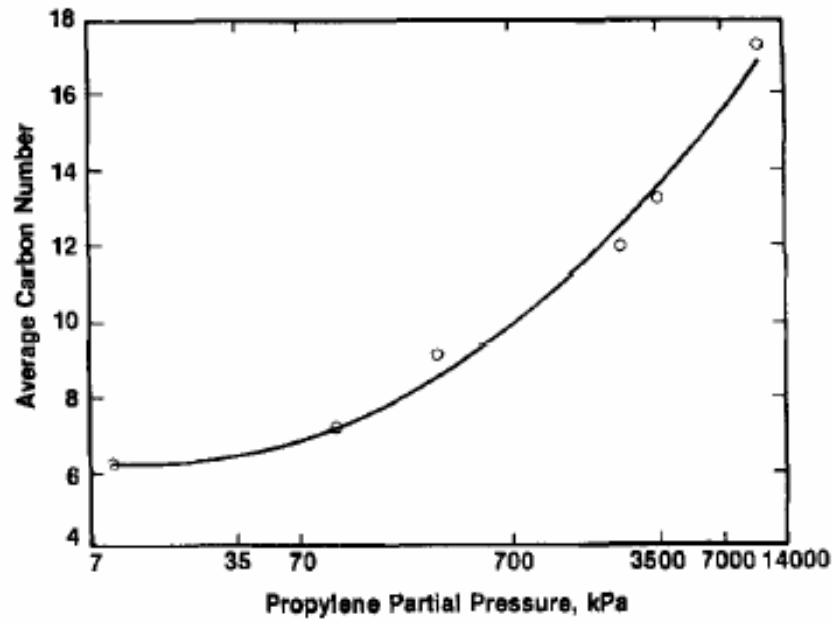

Figure 21: Effect of Propylene Partial Pressure on Average Carbon Number

After hydrotreating the diesel would have the following properties:

Table 22: Diesel Properties[81]:

Specific Gravity	0.78
Pour Point (°C)	<-50
Cetane Number (engine)	56

While the gasoline would have the following properties:

Table 23: Gasoline Properties[82]

Specific Gravity	0.73
Octane	
RON	92
MON	79

POSSIBLE MODIFICATIONS

Modifications to the polymerization model are extensive. The problem is, however, that modifications would require experimentation, and based upon initial findings this would appear to be a waste of money.[83] Essentially, even operating at ideal conditions zeolite polymerization does not compete economically with alkylation. In order to fully describe this process, lots of variables and outputs would have to be added. These include, varying mixture for all four inputs, plus nitrogen, different zeolites, steam generation, and average carbon length distribution. Considering that these all effect each other (a change in zeolite changes the typical structure. A change in typical structure changes chain distribution, which effects octane. All of these changes effect temperature, which requires more propane to quench…etc) it is easy to see how the solution is difficult to obtain, which in the end might be uneconomical relative to alkylation.

DEASPHALTING

PURPOSE

The purpose of propane deasphalting is to separate a mixture of oil and asphalt by using propane as a solvent.

INTRODUCTION

Propane Deasphalting is a process that has been in use since at least the 1930s and was first described extensively by Wilson et al.[84] in 1936. Wilson used propane for liquid-liquid extraction, and stated that propane was superior to other solvents because its solubility properties changed drastically with temperature and pressure. Propane is capable of to removing asphalt,

wax, and resin selectively at different stages, thus making it a good universal solvent. Therefore relatively little has changed for propane deasphalting in means of technology for fifty years. However, within the last two decades there has been increased interest in supercritical fluids for extraction purposes because of their ability to easily mix with extremely viscous fluids, such as oil asphalt mixtures.

The basic propane deasphalting process first combines the oil-asphalt mixture with propane under pressure in a mixer. With thorough mixing two phases form, oil rich and asphalt rich. Depending on the temperature and pressure, these phases could be solid, liquid, vapor, or supercritical fluid. Both Liquid-liquid extraction and supercritical extraction simply flash both streams after initial separation, releasing the propane so it can be recycled. Since the process uses propane as a working fluid, the ratio of propane to oil-asphalt mixture is not of economic concern. Therefore, the ratio is rarely adjusted.

Currently, most of the propane deasphalting systems get their feed from the bottoms of a vacuum distillation tower. Nevertheless, extremely heavy crudes are possible feeds, and have sparked renewed interest, specifically in supercritical extraction.[85]

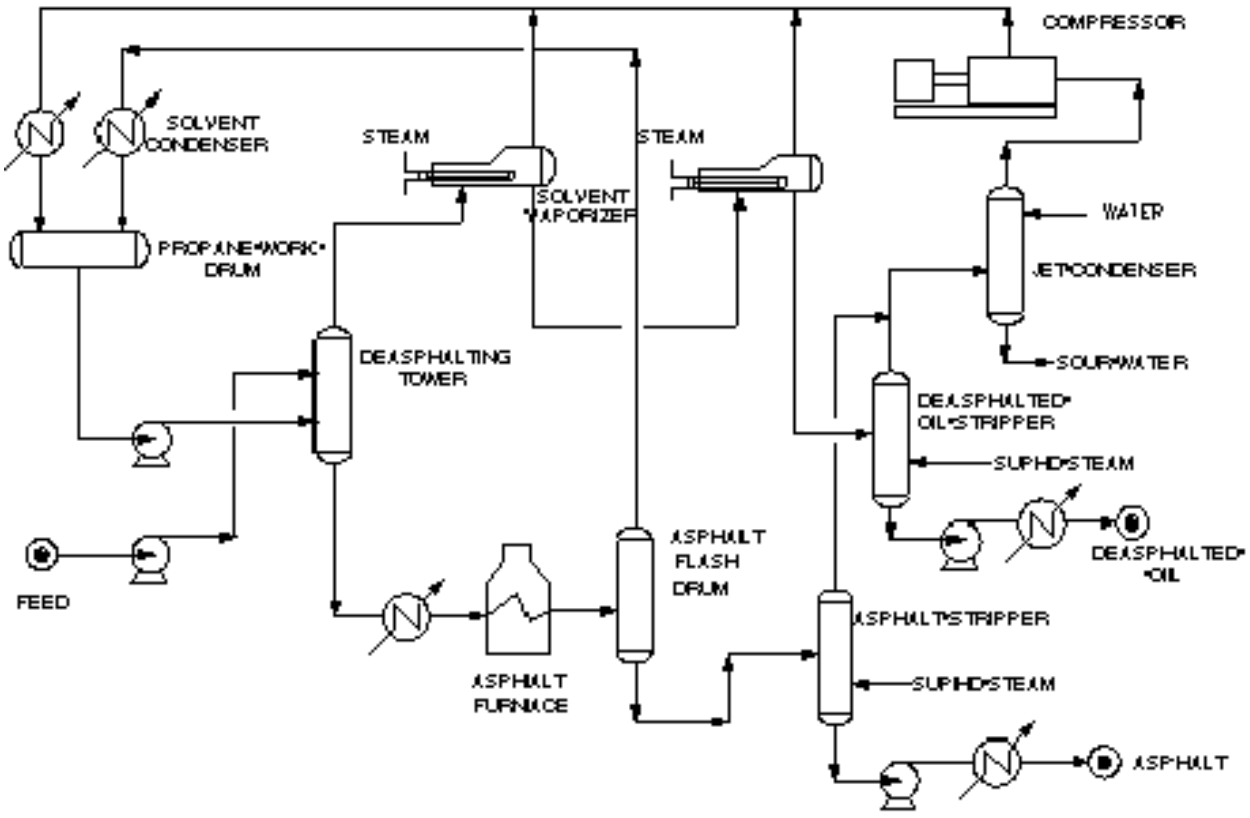

Figure 22: Typical Process Flow Diagram [86]

ASPHALT

Asphalt is a sticky black compound that is a group of aromatic structures of varying size and weight that naturally exist in crude oil. Sold as a raw product, it is used in either paving or roofing applications. The sticky behavior that makes it useful in these applications is directly related to the amount of residual oil left behind after the deasphalting process. Although recently due to high oil prices the economics of leaving costly oil in asphalt has been questioned. Since asphalt is a series of hundreds of different structures, the exact molecular weight is usually given as a distribution that is related to the crude being processed. Therefore, without knowing the distribution of asphalts present in the oil asphalt mixture only generalizations about asphalt in propane behavior can be made.

DEASPHALTED OIL (DAO)

DAO after being the deasphalting process can either be sent to a dewaxing unit (usually incorporated together with the deasphalting unit) or back to be re-cracked. Once again depending on the initial feed, DAO can be rich in light aromatics or saturated hydrocarbons with both being of varying weight and structures.[87]

MODEL

SUB CRITICAL PROPANE DEASPHALTING (LIQUID-LIQUID EXTRACTION)

Wilson et al. were some of the first to develop correlations with crude ternary diagrams. The graphs based on experimental data give the idealized three component system. The problem is that these graphs are specific to pressure and temperature.

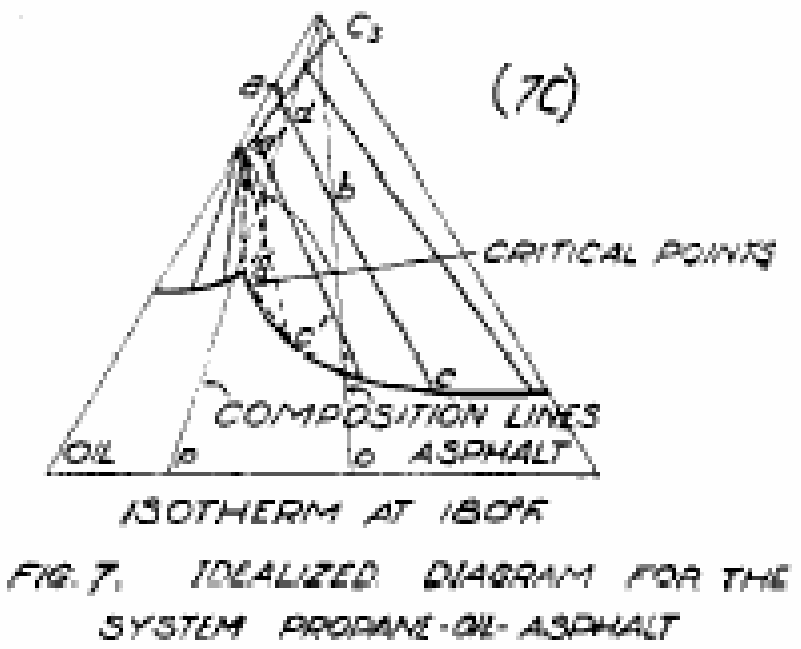

Figure 23: Ternary Diagram -Wilson 1936[88]

Although extensive experimental runs have determined the optimal operating conditions, several attempts to model the liquid-liquid extraction have been proposed. The most popular are models that use the Hildebrand solubility parameter:

$$\delta = \left(\frac{\Delta H - R_g T}{V} \right)^{1/2} \qquad \textbf{Eq. 49}$$

Where

δ = Solubility Parameter [J/mol]

ΔH = Heat of vaporization [J/mol]

R_g = Universal gas Constant [8.314J/mol/K]

T = Temperature [K]

V = molar volume [L/mol]

In order to use this equation several assumptions have been made. It is "assumed that the crude oil is a homogeneous binary mixture of asphalt and the solvent, and that the precipitated asphalt is a homogeneous solid compound." Essentially that the mixture is so well mixed that they don't precipitate individually. "In reality neither assumption is completely true, as neither is the crude oil a homogeneous mixture, nor is the precipitated asphalt a single solid."[89] Therefore, the final model has inherent error. Furthermore, in order to describe all of the various asphalts, it is assumed that the asphalt is polymer like and that the solubility of typical asphalts are similar to that of naphthalene. These assumptions are made so that the following expression can be made.

$$\phi_a^L = \phi_a^S \exp\left[\frac{V_a^L}{V^L} - 1 - \frac{V_a^L}{R_g T} \left(\delta_a - \delta_L \right)^2 \right] \qquad \textbf{Eq. 50}$$

Where

ϕ_a^L = volume fraction of asphalt in liquid phase [vol. %]

ϕ_a^S = volume fraction of solid asphalt = 1

V_a^L = molar volume of asphalt in liquid phase [L/mol]

V^L = molar volume of asphalt-solvent mixture [L/mol]

δ_a = solvent parameter for asphalt [J/L]

δ_L = solvent parameter for liquid phase [J/L]

This equation is justified because it sets the chemical potential of the asphalt in the liquid phase equal to the chemical potential of the solid phase.[90] The range of this model is for the typical range of asphalt in oil mixtures (~10-18%). In developing this equation, researches from the University of Southern California used a type of oil with an average molecular weight of 200 g/mol. They also used a propane to oil-asphalt mixture of 4:1. At 4:1 ratio $V^L \approx 2$ ft^3/mol. In order to obtain the molar volume of asphalt-solvent mixture, the data relating V^L to solvent to oil ratio was extrapolated to include propane. The molar volume of asphalt in liquid phase, V_a^L = 1-4 L/mol, depending on the asphalt oil mixture used, is an experimentally determined value. "Since the results are not very sensitive to V_a^L this quantity can be fixed without great error."[91] Nevertheless, despite the molar volume of the asphalt-solvent mixture changing relative to propane to asphalt ratio, the typical amount of asphalt left in the oil stayed below half a percent.

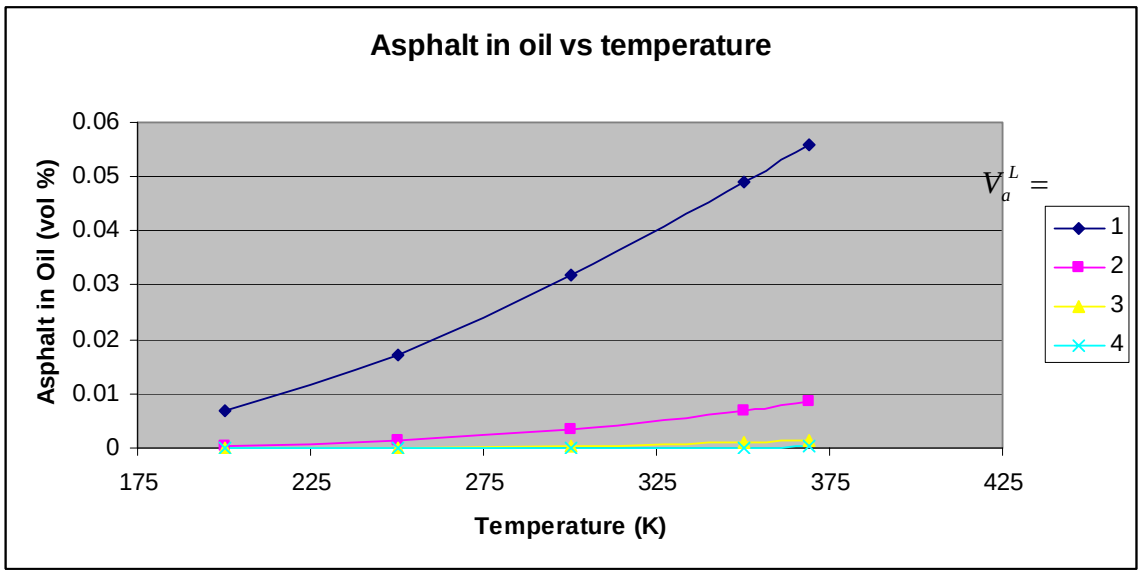

Figure 24: Asphalt in oil vs. Temperature while varying V_a^L

SUPERCRITICAL PROPANE DEASPHALTING

In the late 1970s through the 1980s a series of research projects were conducted in order to develop a model to describe the behavior of propane deasphalting near its critical temperature and pressure. It has been suggested[92] that operating in these conditions is actually more efficient than the sub critical conditions because the solvent rich with oil can be easily regenerated with minor changes in temperature and pressure. In addition to easily regenerating the solvent, operating at a higher temperature allows the normally viscous asphalt to flow much easier, thus reducing pumping cost. Trying to develop a model for the interaction in this supercritical range has been difficult because of the nature of a supercritical fluid. Since supercritical fluids exist above the critical temperature and pressure, distinguishing between a liquid and gaseous phase is difficult. Therefore, equations of state describing this region usually fail. As a direct result, empirical correlations have been used to describe these processes. Specifically these correlations were designed to be useful for asphalt-oil mixtures near 400 K, 55 bar, and a propane to mixture ratio of 4:1.[93] These conditions were selected because they are considered in the optimal range of operating parameters.

POSSIBLE IMPROVEMENTS

Improving the liquid-liquid extraction process model would require adding inputs for the specific asphalt oil mixture being processed. Rather than considering V_a^L and V^L constants, these could be left as inputs. The drawback of this is obviously that it requires more inputs.

As for the other system, supercritical separation is a subject of ongoing research. Thus far the only known way to improve the model's accuracy is to use correlation data for a specific range.

In order to expand both models enough to be useful commercially many more facets need to be explored. For example, depending on design of the facility, the DAO can either go on to become lube oil or sent back to be cracked. If the former happens, then the deasphalting process is part of the recycle stream. Therefore, the amount of asphalt removed from the oil asphalt mixture only needs be equal to the amount of asphalt in the raw crude. If these are set equal to each other then one can calculate the minimum deasphalting process size required.

Another consideration touched out briefly would be maximizing the profit made by selling asphalts of different qualities. As previously mentioned, the amount of other hydrocarbons left in the asphalt product governs the use and price. Although the price of crude is related to the price of gasoline, asphalt, and energy; shifts in market demand could be capitalized on.

CATALYTIC CRACKING

Catalytic cracking is often considered the "workhorse" of most refineries used to convert heavy fuel oils into lighter components, primarily gasoline.[94] While gasoline is the main product of gas oil cracking, another product called "coke" or carbon is also formed. Because coke is undesirable and deactivates the catalyst used in cracking, processes must remove this product from the catalyst to regenerate its capabilities. This has generally been done by burning the deactivated coke in some reactor with superheated air.

Two catalytic cracking processes are being implemented today: Thermofor Catalytic Cracking and Fluid Catalytic Cracking (FCC). Thermofor Catalytic Cracking uses a "moving bed" of catalyst particles.[95] Catalyst that has been regenerated is added to the top of the reactor with the deactivated catalyst passing from the bottom into a kiln. Once burned the reactivated catalyst travels up to the reactor via steam and is stripped from the mixture. The reactivated catalyst then enters back into the reactor where the cracking begins all over again.

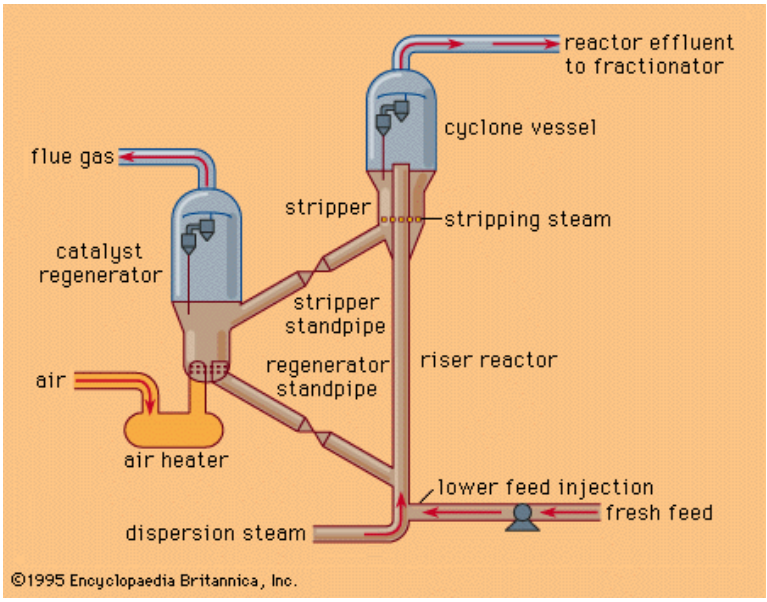

Figure 25: FCC unit[96]

In the FCC unit in Figure 25, the pretreated hydrocarbon enters at the bottom of the riser where it interacts with hot regenerated catalyst. Then, the catalyst and inlet feed pass up the riser as cracking of the gas oil occurs. Depending on the temperature and the space velocity within the riser will yield different cracking yields. At the top of the riser, the mixture is stripped by steam moving the spent catalyst down into a regenerator. The cracked products then enter a cyclone where the rest of the un-stripped catalyst is removed, allowing the products to exit out the top to the fractionator. The stripped catalyst enters a regenerator where it contacts with superheated air. The coke burns in an exothermic reaction where the energy that is released is coupled with the inlet feed at the bottom of the riser.

FIVE-LUMP MODEL

Catalytic cracking involves numerous compounds of varying carbon chains of anywhere from 30-50 carbons. The number of individual compounds present in any given feedstock numbers in the thousands with each compound exhibiting unique cracking kinetics.[97] Therefore, modeling the unit at the molecular level is extremely difficult. To circumvent this issue, models lump specific compounds together and average their kinetic values. Therefore, a five-lump model was assumed with gas oil as A, gasoline as B, LPG as C, dry gas as D, and coke as E.[98] The breakdown of their decay and formation is seen in Figure 26 below with each corresponding

kinetic constant related to each arrow. For example, the arrow from A to B would be a kinetic value of k_{ab}.

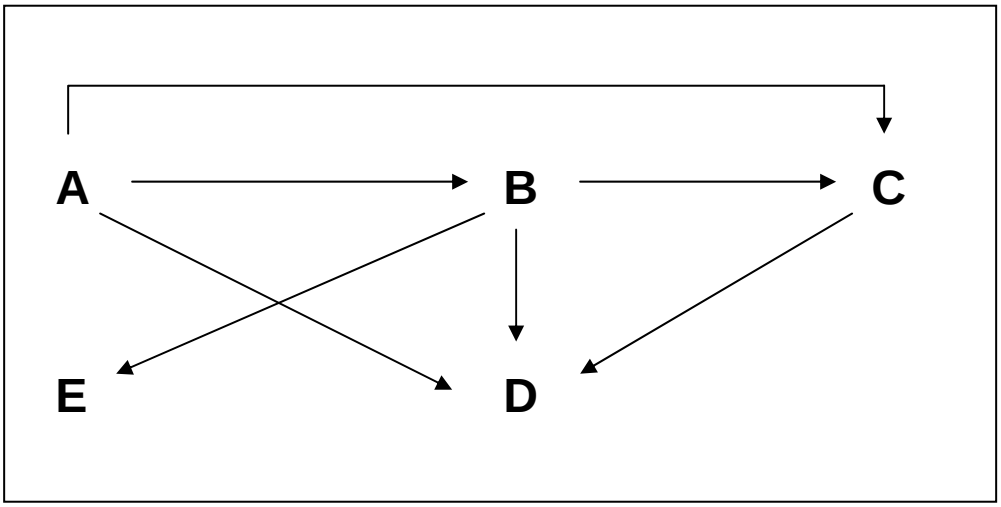

Figure 26: Lumped Parameters: Sequential Method

Since gas oil breaks down into every product and is not formed from any of the products, the order of its decay was assumed to be with respect to 2nd order.[99] The rate kinetics for each product was then assumed to be 1st order. The catalysis de-activation was also assumed to be phi[100]. Therefore, the rate law could be expressed as a function of the kinetic constants, the product yield, and deactivation constant, as seen in Figure 27. Both gasoline and LPG are formed and breakdown into other products, while coke and dry gas do not decay.

$$r_A = -(k_{A-B} + k_{A-C} + k_{A-D} + k_{A-E}) y_A^2 \Phi$$

$$\Phi = e^{-k_d t_c}$$

Figure 27: Rate Constants

PFR

To calculate the yield fractions of the cracked gas oil, the catalytic cracking unit was modeled as a one-dimensional plug flow reactor (PFR). The PFR was assumed to have negligible axial and radial dispersion. Other assumptions are[101]:

1) Adsorption on the inside of the catalyst is negligible
2) The coke has the same properties as the specific catalyst
3) Coke deposited on the catalyst will not affect the flow of fluid
4) Adiabatic walls

While some models use PFRs in series with CSTRs, a single PFR was modeled because the kinetic values were calculated by a Runge Kutta Method that minimized the sum of the squares between experimental and calculated product yields. Therefore, experimental data from a Microactivity Test (MAT) reactor was used to minimize the objective function below[102]

$$\frac{dy_i}{dz} = \frac{1}{WHSV}\left(\frac{\rho_L}{\rho_C}\right) * r_i \qquad \textbf{Eq. 51}$$

where WHSV is the weighted hour space velocity, r_i the rate of the i^{th} component, and ρ_L, ρ_C, the gas oil density and catalyst density respectively (kg/m^3).

The kinetic values that were calculated from the minimization of Equation 51 are tabulated below. Since these values are dependent on the specific feedstock properties, it is expected to see different k values for differing gas oils. The kinetic values are also dependent upon the temperature within the riser. Since the activation energies were calculated, kinetic values for 480 and 520 ºC were also calculated.

Kinetic Parameters for each Feedstock at 500 °C			
	A	B	C
k_d	1481.85	1785	1905.24
k_{ab}	3370.6	3171	2907.18
k_{ac}	510.88	491.74	477.02
k_{ad}	10.76	75.3	86.06
k_{ae}	390.03	442.96	540.67
k_{bc}	181.8	154.98	101.33
k_{bd}	20.89	25.46	29.38
k_{be}	0.75	0.915	1.06
k_{cd}	286.58	323.83	353.92

Figure 28: Kinetic values at 500 °C [103]

Exploring the range of kinetic values shows k_{ab} is substantially larger than any other kinetic constant. This suggests that gas oil break down can best be explained kinetically by the formation of gasoline. Gasoline yield is thus then dependent upon how strongly the gasoline degrades into LPG, dry gas, and coke. Since k_{ae} is significantly smaller than the other degraded kinetic values, gasoline can be assumed to breakdown into only LPG and dry gas.

Using the mass balance of Equation 51, the concentration profiles were calculated numerically using Euler's method, as shown below:

$$\textit{Euler's Method} \qquad C_i = C_{oi} + \frac{dC_i}{dz} dz \qquad \textbf{Eq. 52}$$

where the initial concentration of A was 1, with every product having 0 as their initial concentrations. The "dz" was the specified step change that was assumed to be .001 m. The dC_i/dz term was the specific rate for the i^{th} component.

While the concentration profiles showed 70-80% yields at .005 m, the real value was probably substantially greater. However, with no known densities of the catalyst and inlet fluid, because they were specific for the unique catalyst by,[104] the mass balance did not include them. Since errors may occur because of this deviation, future work should include the specific densities.

BLENDING

PRODUCT BLENDING

Blending units take the intermediate streams produced by refinery units and produce finished products that meet given specifications. By using blending, a refinery can adapt more quickly to different market demands and price levels. A blending model is used to optimize the use of the intermediate streams to meet demands and maximize profit. Increasing the accuracy of blending models will contribute to increasing the refinery's profit by increasing the optimization of the intermediate streams that the refinery produces.

The products that a refinery produces include different grades of gasoline, diesel, jet fuel, fuel oils, and lube oils. These products have different specifications that depend on different properties. The properties that are used in meeting specifications include octane, vapor pressure, viscosity, aniline point, pour point, cloud point, flash points, and diesel index. In gasoline, the octane, the vapor pressure, and the maximum amount of gasoline additives used are important specifications. Two major additives are n-butane and ethanol, which is currently replacing methyl tert-butyl ether (MTBE) as the primary octane-enhancing additive in the United States.

Most of the important properties for refinery products do not blend linearly, and blending indices are used to linearize the system of equations to reduce the computational time required. The refinery model presented in this paper uses a linear blending model, based on volume percent weighted averages. Non-linear models are also discussed for some properties. Non-linear models are becoming more feasible as the capabilities of modern computers increase. Non-linear models may offer increased accuracy over linear models, leading to greater blending optimization and refinery profit.

BLENDING MODEL

The current refinery model has thirty-five petroleum streams coming into the blending section of the refinery from thirteen process units. Thirty of these streams are blended into gasoline, and the other five streams create other products, which are liquefied petroleum gas (LPG), coke, lube oil, asphalt, and wax.

For each of the gasoline streams, the mass flow rate, API gravity, octane numbers (MON, RON), and Reid Vapor Pressure (RVP) are known. From these values, the volumetric flow rates and vapor pressure blending index are calculated. Two grades of gasoline are produced: normal grade (87 octane) and premium grade (91 octane). Both grades have the Environmental Protection Agency mandated constraint on RVP of 8.7 psi for the summer months, and 12 psi for the winter months. They also have the same constraint on total n-butane content of 8%. The other inputs into the gasoline blending model are the predicted market demands and market prices for the two grades of gasoline.

With these inputs, the blending model optimizes the amount of each of the thirty streams that blends to produce the two grades of gasoline. The maximized objective function is the profit, and the constraints are the component mass balances, and the gasoline specifications (octane, RVP, and maximum n-butane content). The octane requirement is calculated by using a volume percent weighted average for both the MON and RON, and averaging the resulting MON and RON. The RVP requirement is calculated by using a volume percent weighted average of the vapor pressure blending index and comparing this to the vapor pressure blending index of the required RVP. The n-butane content restriction is met by requiring the volume percent of n-butane to be less than or equal to the maximum value.

The process unit models currently in use do not produce enough information to accurately blend other products, such as diesel, fuel oils, or lube oils. For diesel, the aniline point and the API gravity are required to calculate the diesel index. The current models do not provide aniline points. For fuel oils, properties such as flash point, pour point, and cloud point are important. For lube oils, pour point, cloud point and viscosity index are important parameters. The current models do not provide viscosity, flash point, or cloud point, so fuel oils and lube oils could not be mixed. If this data were to be added in future work, the model could easily be expanded to include these products. The same blending method used for the gasoline blending could be used, substituting the important specifications in place of the gasoline octane and RVP specifications.

OCTANE NUMBER

Octane number is an important characteristic of fuels used in spark engines, such as gasoline. It represents the antiknock characteristic of a fuel. There are two methods used to determine the octane number of a fuel. The motor octane number (MON) of a fuel is measured under road conditions, and the research octane number (RON) is measured under city conditions. The average of the MON and RON is the posted octane number that consumers see at the gas pump, and is the specification that must be met.

The octane number of a fuel is highly dependent on the chemical structure of the individual components in the mixture, and affected by interaction between molecules. Due to these properties, octane numbers blend nonlinearly. Weighted averages can be used when the contribution of each component is less than approximately 15% of the total volume, without introducing a large amount of error. Many blending approaches have been developed, including a blending index for the research octane number given by the analytical relation below:

$$BI_{RON} = 3.205 + (0.279 * EXP(0.031 * RON)) \quad \textbf{Eq. 53}$$

After the octane numbers have been converted to the octane blending index, they blend linearly, and the resulting research octane number is obtained by solving the equation above for RON.

VAPOR PRESSURE

The Reid Vapor Pressure is a measure of a petroleum mixture's vapor pressure at 100°F, and is used to determine the volatility of the mixture. It differs from the mixture's true vapor pressure at temperatures other than 100°F, and may include measurement error from the equipment used to measure it. RVP is used to standardize volatility measurements. It does not blend linearly, and a blending index is used to linearize blending calculations. Vapor pressure blending index (VPBI) determined from RVP by:[105]

$$VPBI = (RVP)^{1.25} \quad \textbf{Eq. 54}$$

A theoretical model for vapor pressure blending can be determined from thermodynamics, and is feasible for the case in which the input streams from the refinery units have relatively constant compositions. The composition of the petroleum mixture would have to be known. In refineries, the composition of the purchased crude oils changes, which changes the composition of the

inputs and outputs of the refinery process units, despite blending different crude oils to keep the blend entering the refinery relatively constant. This provides the blending units, on the very end of the refinery, with inputs of varying composition.

For the model to be developed, the fugacity of each component, relative to the interactions with the other components in the mixture, would be calculated, and then the overall fugacity of the system would be the sum of the fugacities of each component. Once the true vapor pressure from this method was known, the RVP of the mixture would be determined by solving for the true vapor pressure at 100°F.

LIQUID VISCOSITY

Liquid viscosity can be estimated using empirical correlations, and most correlations estimate liquid viscosity as only a function of temperature, because most applications for which viscosities are important are at low to moderate pressure. Viscosity is inversely proportional to temperature. Eyring developed the following semi-theoretical model from thermodynamics and tuned the coefficients using experimental data.[106]

$$\mu = \frac{N_A h}{V} * \exp\left(\frac{3.8 T_b}{T}\right) \qquad \textbf{Eq. 55}$$

Where:

μ is the absolute liquid viscosity in poise at temperature T;

T is the temperature in Kelvin;

T_b is the normal boiling point in Kelvin;

h is Planck's constant (6.624E-27 g*cm2/s); and

N_A is Avogadro's number (6.023E23 gmol-1).

For petrochemicals, an empirical correlation has been developed that gives the liquid viscosity within +-5% of the actual value. Five experimentally determined parameters (A, B, C, D, and E) are used. This data is available from the American Petroleum Institute's Technical Databank (API-TDB).[107]

$$\mu = 1000 * \exp\left(A + \frac{B}{T} + C \ln T + D * T^{E} \right)$$ **Eq. 56**

For defined liquid mixtures, the following mixing rules are recommended in the API-TDB and Design Institute for Physical Properties (DIPPR) manuals:[108]

$$\mu_m = \left(\sum_{i=1}^{N} x_i \mu_i^{1/3} \right)^3 \text{ for liquid hydrocarbons}$$ **Eq. 57**

$$\ln \mu_m = \sum_{i=1}^{N} x_i \ln \mu_i \text{ for liquid nonhydrocarbons}$$ **Eq. 58**

Where:

μ_m is the absolute viscosity of the mixture;

μ_i is the absolute viscosity of component i, with the same units as μ_m is desired in;

x_i is the volume fraction of component i.

For liquid petroleum fractions of unknown compositions, an experimental data point can be taken for the viscosity at 100°F, and then the following correlation can be used:[109]

$$\log_{10}[\nu_T] = A\left(\frac{311}{T} \right)^{B} - 0.8696$$ **Eq. 59**

$$A = \log_{10}(\nu_{100}) + 0.8696$$
$$B = 0.28008 * \log_{10}(\nu_{100}) + 1.8616$$

Where:

T is the liquid's temperature in Kelvin;

ν_{100} is the viscosity data point taken at 100F, in cSt;

ν_T is the viscosity at temperature T, in cSt.

Once the viscosity is known, the viscosity-blending index can be calculated using the correlation below, developed by the Chevron Research Company. Once the blending index is known, the viscosity index of a mixture can be determined using the volume-weighted averages of the blending indices of the constituents.[110]

$$BI_{\nu} = \frac{\log_{10} \nu}{3 + \log_{10} \nu}$$

$$BI_{\nu,mix} = \sum x_{\nu i} BI_{\nu,i}$$ **Eq. 60**

Where:

ν is the kinematic viscosity in cSt;

$BI_{v,i}$ is the viscosity blending index of component I;

$x_{v,i}$ is the volume fraction of component i.

ANILINE POINT

The aniline point is the minimum temperature at which equal volumes of the petroleum fraction and aniline are completely miscible. Higher aromatic content of the petroleum fraction lowers the aniline point. Due to this relation, the aniline point, combined with the specific gravity of the mixture, can be used to calculate the percent aromatic content of a petroleum fraction.[111]

$$\%A = 692.4 + 12.15(SG)(AP) - 794(SG) - 10.4(AP)$$ **Eq. 61**

Where:

%A is the percent aromatic content;

SG is the specific gravity;

AP is the aniline point in °C.

The Linden Method can be used to determine the aniline point from the API gravity and the mid boiling point of the mixture. The aniline point does not mix linearly, and a blending index is defined by the Chevron Research Company in the second equation below:[112]

$$AP = -183.3 + 0.27(API)T_b^{(1/3)} + 0.317T_b$$ **Eq. 62**

Where:

AP is the aniline point in °C;

T_b is the mid boiling point in Kelvin;

API is the API gravity.

$$BI_{AP} = 1.124[\exp(0.00657\,AP)]$$ **Eq. 63**

POUR POINT

"The pour point of a petroleum fraction is the lowest temperature at which the oil will pour or flow when it is cooled without stirring under standard cooling conditions… When temperature is less than pour point of a petroleum product it cannot be stored or transferred through a pipeline."

Pour point depressant additives are used in producing engine oils, and can achieve pour points as low as -25 to -40°C. Pour point depressants inhibit the growth of wax crystals in the oil.

The pour point of a petroleum fraction can be estimated from viscosity, average molecular weight, and specific gravity using the following empirical equation, which was developed with data from over 300 petroleum fractions:[113]

$$T_p = 130.47\left[SG^{2.970566}\right] * \left[M^{(0.61235-0.47357\,SG)}\right] * \left[\nu_{100}^{(0.310331-0.32834\,SG)}\right]$$ **Eq. 64**

Where:

T_p is the pour point in Kelvin

M is the molecular weight

υ_{100} is the kinematic viscosity at 100°F

The pour point of petroleum mixtures does not blend linearly, and a pour point blending index is used to linearize the system. The pour point blending index is related to the pour point temperature by the following relation:[114]

$$BI_p = T_p^{\left(\frac{1}{0.08}\right)}$$ Where T_p is the pour point in Kelvin. **Eq. 65**

$$BI_{p,mix} = \sum x_{vi} BI_{p,i}$$ **Eq. 66**

CLOUD POINT

"The cloud point is the lowest temperature at which wax crystals begin to form by a gradual cooling under standard conditions… Cloud points are measured for oils that contain paraffins in

the form of wax." For light fractions that do not contain waxy paraffins, such as gasoline, cloud point data is unavailable.

The cloud point is generally a few degrees Celsius lower than the pour point, although no consistent variation between the two exists. The cloud point, like the pour point, does not blend linearly, and a blending index is used to linearize the system. The relation shown below is the same as the pour point relation, but with a different exponent.[115]

$$BI_{CL} = T_{CL}^{\left(\frac{1}{0.05}\right)}$$ Where T_{CL} is the cloud point in Kelvin. **Eq. 67**

A volume-weighted average is used to find the cloud point blending index of a mixture. (Riazi, 136)

$$BI_{CL,mix} = \sum x_{vi} BI_{CL,i}$$ **Eq. 68**

FLASH POINT

The flash point is the lowest temperature at which the petrochemical mixture can form an ignitable mixture with air. The flash point can be determined experimentally, and does not blend linearly. The following correlation can be used to calculate the flash point blending index from the flash point temperature.[116]

$$\log_{10} BI_F = -6.1188 + \frac{2414}{T_F - 42.6}$$ **Eq. 69**

Once the flash point blending index is known for the compounds in a mixture, the flash point blending index can be determined from a weighted average of the blending indices of the components.[117]

$$BI_{F,mix} = \sum x_{vi} BI_{F,i}$$ **Eq. 70**

DIESEL INDEX AND CETANE INDEX

The diesel index and cetane index measure the favorability of auto-ignition in a petroleum mixture. This property is essential for diesel engines. The diesel index can be calculated from the API gravity and the aniline point using the following empirical correlation:[118]

$$DI = \frac{(API)(1.8AP + 32)}{100} \qquad \textbf{Eq. 71}$$

Where:

AP is the aniline point in °C;

API is the API gravity

The cetane index can then be found from the diesel index using the following empirical correlation:[119]

$$CI = 0.72DI + 10 \qquad \textbf{Eq. 72}$$

Once either the diesel or cetane indexes are known, a final diesel product can be blended.

REFINERY MODELING

After all of the refinery unit models had been developed, they were combined together in an overall refinery model. The refinery model was used to determine the optimal crude purchases and process variables to obtain the maximum profit from producing final products, given crude prices and availability, and product prices and demands. All of these parameters are readily changeable in the Excel spreadsheet used for the optimization.

The optimization was initially attempted using Excel Solver. The variables changed were the crude purchases and process variables. The process variables included unit temperatures, pressures, input stream ratios, and blending ratios. The objective function was the total profit, which was obtained from the following equation:[120]

$$\text{Maximum Profit} = \sum_{t \in T} \sum_{c \in C_p} MANU_{c,t} * cp_{c,t} - \sum_{t \in T} \sum_{c \in C_o} AC_{c,t} * co_{c,t} - \sum_{t \in T} \sum_{c \in C_p} AL_{c,t} * cl_{c,t} \qquad \textbf{Eq. 73}$$

The first term corresponds to the products that are being produced during the model run time. The default time parameter used in the model is one month, assuming a constant demand over that month. However, this equation spans every point in the time frame, allowing for varying production and demand. The second summation spans the different products that are produced. $MANU_{c,t}$ corresponds to the amount of product c produced at time t. The variable $cp_{c,t}$ corresponds to the price of product c at time t.

The second term corresponds to the crude oil costs. This model also assumes constant crude oil costs, but the summation terms can be used for varying amounts and prices over time. $AC_{c,t}$ corresponds to the amount of crude oil type c purchased at time t. The variable $co_{c,t}$ corresponds to the price of oil c at time t.

The third term corresponds to the demand penalty, which reduces the total profit if the demand is not met. This term corresponds to penalties that would be written into contracts with purchasers of the refinery's products. This also varies with time and the product. $AL_{c,t}$ corresponds to the amount of crude oil type c purchased at time t. The variable $cl_{c,t}$ corresponds to the price of oil c at time t.

Product specifications were incorporated into the model as constraints. For each product, there was a constraint equation that forced the solution to be within specifications for properties. For gasoline, these properties were posted octane number, Reid vapor pressure, and maximum n-butane content.

In addition to specification restraints, there was a demand constraint prohibiting the refinery from producing more product than could be sold. Mass balances for the blending mixtures were enforced as constraints, to prevent Solver from using more of an intermediate component than the refinery is able to produce. The mass balances took the form of:

$$0 \leq (m_{i,normal}+m_{i,premium}) \leq m_{i,available} \qquad \textbf{Eq. 74}$$

Where: $m_{i,normal}$ is the mass of component i in normal grade gasoline

$m_{i,premium}$ is the mass of component i in premium grade gasoline

$m_{i,available}$ is the mass of component i produced by the refinery units

Possible ranges for process variables were inputted into Solver as constraints as well. Temperatures, pressures, and mixing ratios all were kept within normal operating conditions.

For the blending alone, there were thirty components available for blending into both grades of gasoline. This formed a matrix of 2 x 30 options for blending gasoline. There were sixty corresponding mass balance restrictions.

When this system was initially attempted to be solved using Excel Solver, it would time out. When the time limit was increased, it would still not converge. The crude selection has the most effect on the overall profit, due to the large penalties associated with not meeting demand. Solver is capable of solving the system of equations when the crude selection is not a part of the system. However, this is not an acceptable solution because the determination of the crude oil purchases is the aim of this project.

A macro was written in Excel using the Visual Basic software package included in standard versions of Excel. This macro varies the crude selection across a specified range. For each crude selection, Solver is invoked to find the maximum profit possible for that selection by optimizing the process variables and blending parameters. This data is then recorded in Excel, and the macro highlights the optimal crude selection obtained in a specially marked table.

The crude selection is varied by using three nested loops that vary the three crude selections across the specified ranges. This ensures that every possible combination of crudes within the ranges is considered by the optimization. The step size determines the maximum error that will be associated with the final optimized value. The larger the step size, the faster a solution is reached, but the less accurate the solution is. While this macro works to obtain the optimal crude selection, it is not the best optimization method possible.

This macro could be improved by implementing a smarter search pattern for the optimal solution. The current search pattern is to entirely cover the range of possible solutions given a step size. The step size has to be relatively large (10,000-20,000 barrels) for the solution to

converge within a few hours. A smarter search pattern would be to use a numerical equivalent to a derivative, such as a modification of Newton's difference quotient, as given below:

$$\frac{\Delta \text{Profit}}{\Delta \text{x}} = \frac{f(x+h) - f(x-h)}{2h} \approx f' \qquad \textbf{Eq. 75}$$

Where f is the Profit function

x is one of the crude oil selections

h is a small step size, such as 1 barrel

Once this has been used to determine the direction of increasing profit for the three crude oil parameters, a step size α would either be added or subtracted from the current amounts of crude oil selected, and the iteration followed once again, until f' changed less than a pre-set value. This method should converge more quickly to a solution than the currently implemented method, although it will also take a considerable amount of time to find a solution. Six function calls to Solver are required for each calculation of the crude oil selection gradient.

The current model implemented in Excel is capable of determining the optimal short-term crude purchasing strategy for a refinery, given the constraints of constant short-term prices and demands. The current processing time required to find the optimal purchasing slate to within 1000 barrels is several days, but for once a month running, this is acceptable.

RESULTS AND CONCLUSIONS

Running the refinery model generated a maximum profit of $21 per barrel of crude processed. This profit corresponded to one of the situations in which the demand was exactly met. A step size of 25,000 barrels was used. This large step size was selected due to the necessity of producing this result in a short amount of time. Thus, the crude selections below may be off of the true optimal values by a maximum of 25,000 barrels per month. The model inputs and the optimized crude selection and profit results are summarized in the tables below. If this model was to run with more accurate inputs, and had adequate run time available, it is capable of producing the optimal result with a much smaller error than 25,000 barrels per month.

Table 24: Model Inputs

Variable	Value
Crude A price (Australia)	$71.88 / barrel
Crude B price (Kazakhstan)	$72.00 / barrel
Crude C price (Saudi Arabia)	$71.20 / barrel
Regular gasoline price	$2.75 / gallon
Premium gasoline price	$3.00 / gallon
Regular gasoline demand	310,000 bbl / month
Premium gasoline demand	124,000 bbl / month

Table 25: Model Results

Maximum Profit	$21 per barrel
Crude A purchased	150,000 bbl / month
Crude B purchased	150,000 bbl / month
Crude C purchased	300,000 bbl / month

All major refinery inputs and outputs are accounted for in this refinery model, providing a good approximation of how a refinery works and processes oil. The shortcomings of this model, caused by the time constraints in development, are outlined below in the Future Work section. The implementation of these recommendations would improve the model accuracy and make it more suitable for industrial use.

FUTURE WORK

Each model can improve by expanding pseudo components into a narrower range, as well as exploring recommendations at the end of each unit section. The current model is limited to solving for demand on a one month basis. Forecasting demand and maximizing the profit over an extended time would give a more realistic refinery planning model. This implies that storage of products and blending over time would have to be explored as well.

Future models would also have to implement a greater product selection. Currently gasoline is the only major product that is being sold. Adding lube oils, fuel oils, diesels, solvents, and other typical chemical feedstocks would strengthen the model's versatility. This means getting data for aniline points, pour points, and diesel indexes, to name a few, necessary for blending properties.

Finally, future work should address the current uncertainty in prices as well as risk associated with supply of the crude products. Risk and uncertainty are an intricate part of oil planning. Each addition will therefore address specific downfalls of the current refinery model and create a more sound application for the maximization of refinery planning.

REFERENCES

Note: In-text numbers correspond to the footnotes found at the end of this section.

1. Aleksandrov, A.S. et al. Kinetics of low-temperature n-pentane isomerization over NIP-66 catalyst. Khimiya i Teckhnologiya Topliv i Masel. No. 10, pp. 5-8, October, 1976.

2. Alkylation of Isobutane with C3-C5 Olefins To Produce High-Quality Gasolines: Physicochemical Sequence of Events Albright, L. F. Ind. Eng. Chem. Res.; (Article); 2003; 42(19); 4283-4289.

3. Alkylation of Isobutane with C3-C5 Olefins: Feedstock Consumption, Acid Usage

4. Alkylate Quality for Different Processes Albright, L. F. Ind. Eng. Chem. Res.; (Article); 2002; 41(23); 5627-5631

5. Asphalt flocculation and deposition: I. The onset of precipitation AIChE Journal Volume 42, Issue 1, Date: January 1996, Pages: 10-22 Hossein Rassamdana, Bahram Dabir, Mehdi Nematy, Minoo Farhani, Muhammad Sahimi

6. Burisan, N.R., N.K. Volnukhina, A.A. Polyakov, and I.S. Fuks. Kinetic relationships in the low-temperature isomerization of n-butane. Khimiya i Teckhnologiya Topliv i Masel. No. 10, pp. 6-8, October, 1972.

7. C. S. Laxminarasimhan, R. P. Verma, P. A. Ramachandran. Continuous lumping model for simulation of hydrocracking. AIChE Journal. 42(9) 2645-2653 (1996).

8. Characterizing Hydrocarbon Plus Fractions. Whitson, Curtis H.. Society of Petroleum Engineers of AIME. 1983.

9. Cheng-Lie Li, Zhe-Lin Zhu. Network of n-Hexane isomerization over Pt/Al2O3 and Pd/HM catalysts. Fuel Science and Technology Int'L. v. 9 n. 9. Jan. 01 1991 pg 1103-1122.

10. Conversion of propylene and butylene over ZSM-5 catalyst AIChE Journal Volume 32, Issue 9, Date: September 1986, Pages: 1526-1531 S. A. Tabak, F. J. Krambeck, W. E. Garwood

11. Conversion Process. Petroleum Refining. Ed. Pierre Leprince. Institut Francais du Petrole Publications. 1998 Editions Technip, France.

12. Correlation of pour point of gas oil and vacuum gas oil fractions with compositional parameters. Energy & Fuels, 3(1) 15-20 (1989).

13. Encyclopedia of Chemical Processing and Design. 62 Vent Collection System, Design and Safety to Viscosity-Gravity Constant, Estimation. Ed. John McKetta. 1998 Marcel Dekker, Inc. New York, NY.

14. FCC Unit (http://www.plantech.or.kr/diagram/pc_refinery/refinery_t2.gif)

15. Firoozabadi, A., and Katz, D. L. 1978. Predicting phase behavior of condensate/crude-oil systems using methane interaction coefficients. Journal of Petroleum Technology 30(11):1649–1655.

16. Galiasso et al., Hydrotreat of Light Cracked Gas Oil, Heinz Heinemann, copyrighted 1984, pg 145-153

17. Gary, J.H. and G.E. Handwerk. Petroleum Refining: Technology and Economics. Marcel Dekker Inc: New York, 2001, 121-141. and A.V. Mrstik, K.A. Smith, and R.D. Pinkerton, Advan. Chem. Ser. 5 , 97. 1951.

18. Hagelberg, P. et. al. Kinetics of catalytic cracking with short contact times, Applied Catalysis A: General 223 (2002) 73-84

19. Han, In-Su, Dynamic modeling and simulation of a fluidized catalytic cracking process. Part I: Process modeling, Chemical Engineering Science 56 (2001) 1951-1971

20. Hydrocracking PFD, www.isa.org

21. Hydrotreating Unit PFD, http://www.osha.gov/dts/osta/otm/otm_iv/otm_iv_2fig25.gif

22. Interfacial Area of Dispersions of Sulfuric Acid and Hydrocarbons David J. Ende, Roger E. Eckert, Lyle F. Albright Ind. Eng. Chem. Res.; 1995; 34(12); 4343-4350.

23. Juarez-Ancheyta, Jorge, et. al. Estimation of Kinetic Constants of a Five-Lump Model for Fluid Catalytic Cracking Process Using Simpler Sub-models, Energy & Fuels 2000, 14, 1226-1231

24. Krishna, R., G. C. Joshi, R. C. Purohit, K. M. Agrawal, P. S. Verma, S. Bhattacharjee

25. LIQUID PROPANE Use in Dewaxing,Deasphalting, and Refining Heavy Oils Robert E. Wilson, P. C. Keith, , Jr. R. E. Haylett Ind. Eng. Chem.; 1936; 28(9); 1065-1078.

26. May 4, 2006. http://jechura.com/ChEN409/11%20Alkylation.pdf CO School of Mines

27. May 4, 2006. http://www.prod.exxonmobil.com/refiningtechnologies/pdf/AIChE2002SpringAlky.pdf

28. May 4, 2006. http://www.prod.exxonmobil.com/refiningtechnologies/pdf/AlkyforWR02.pdf

29. May 4, 2006. http://www.scielo.br/scielo.php?script=sci_arttext&pid=S0104-66322000000300012&lng=pt&nrm=iso – PDF

30. Meyers, Robert A. Handbook of Petroleum Refining Processes. 3rd edition. McGraw-Hill: NewYork, 2004, 14.35.

31. Moulton, R.W. and V.K. Loop. Compostion of Petroleum Waxes from western crudes. Petroleum Refiner, 24(4) 121-3 (1945).

32. Nelson, W.L. Oil and Gas Journal. 65 (26) 84-85 (1967).

33. NPRA "Diesel Sulfur" www.npradc.org/issues/fuels/diesel_sulfur.cfm

34. Petroleum Handbook, The. Sixth Edition. Elsevier Science Publishers. 1983. p 276-283.

35. Phase equilibria in supercritical propane systems for separation of continuous oil mixtures Maciej Radosz, Ronald L. Cotterman, John M. Prausnitz Ind. Eng. Chem. Res.; 1987; 26(4); 731-737.

36. Pongsakdi, Arkadej, et. al. Financial Risk Management in the Planning of Refinery Operations. International Journal of Production Economics. Accepted for publication, 20 April 2005.

37. Properties of gases and liquids, the. Reid, Robert C.

38. R. DeBiase and J. D. Elliott, "Recent Trends in Delayed Coking," NPRA Annual Meeting, San Antonio, March 1982.

39. Riazi, M.R. Characterization and Properties of Petroleum Fractions. West Conshohocken, PA: ASTM International, 2005., p. 335

40. Solvent Dewaxing. Oil and Gas Journal. April 3, 1961. page 127.

41. Stangeland, B. E., "Kinetic Model for Prediction of Hydrocracker Yields," Znd. Eng. Chem. Proc. Des. Deu., 13(1), 72 (1974).

42. Sulfur Removal, http://library.wur.nl/wda/abstracts/ab3328.html

43. Tabak, S.A., U.S. Patent 4,254,295 (1981)

44. The kinetics of alkylation of isobutane with propylene AIChE Journal Volume 18, Issue 4, Date: July 1972, Pages: 698-705 J. Randolph Langley, Ralph W. Pike

45. Upson, L. Lawrence and Reagan, William J., et. al. The Art of Evaluating Laboratory Fixed Bed and Fixed Fluid Bed Catalytic Cracking Data, unpublished, January 2005

46. Weekman, Vern W. Jr., Lumps, Models, and Kinetics in Practice, The American Institute of Chemical Engineers 1979, No. 11, Vol 75.

---

[1] NPRA "Diesel Sulfur" www.npradc.org/issues/fuels/diesel_sulfur.cfm

[2] Sulfur Removal, http://library.wur.nl/wda/abstracts/ab3328.html

[3] Hydrotreating Unit PFD, http://www.osha.gov/dts/osta/otm/otm_iv/otm_iv_2fig25.gif

[4] Galiasso et al., Hydrotreat of Light Cracked Gas Oil, Heinz Heinemann, copyrighted 1984, pg 145-153

[5] Galiasso et al

[6] Galiasso et al

[7] Galiasso et al

[8] Galiasso et al

[9] Gary, J.H. and G.E. Handwerk. Petroleum Refining: Technology and Economics. Marcel Dekker Inc: New York, 2001, 121-141. and A.V. Mrstik, K.A. Smith, and R.D. Pinkerton, Advan. Chem. Ser. 5 , 97. 1951. 80

[10] Gary and Handwerk, 71

[11] R. DeBiase and J. D. Elliott, "Recent Trends in Delayed Coking," NPRA Annual Meeting, San Antonio, March 1982.

[12] Gary and Handwerk, 71

[13] Gary and Handwerk, 71

[14] *Petroleum Handbook, The*. Sixth Edition. Elsevier Science Publishers. 1983. p 276-283.

[15] *Conversion Process*. Petroleum Refining. Ed. Pierre Leprince. Institut Francais du Petrole Publications. 1998 Editions Technip, France.

[16] *Encyclopedia of Chemical Processing and Design.* 62 Vent Collection System, Design and Safety to Viscosity-Gravity Constant, Estimation. Ed. John McKetta. 1998 Marcel Dekker, Inc. New York, NY.

[17] *Conversion Process*.

[18] *Encyclopedia of Chemical Processing and Design. 62*

[19] *Conversion Process*.

[20] *Encyclopedia of Chemical Processing and Design. 62*

[21] *Encyclopedia of Chemical Processing and Design. 62*

[22] *Petroleum Handbook, The*. Sixth Edition. Elsevier Science Publishers. 1983. p 276-283.

[23] *Encyclopedia of Chemical Processing and Design. 62*

[24] *Encyclopedia of Chemical Processing and Design. 62*

[25] *Encyclopedia of Chemical Processing and Design. 62*

[26] *Characterizing Hydrocarbon Plus Fractions.* Whitson, Curtis H.. Society of Petroleum Engineers of AIME. 1983.

[27] *Characterizing Hydrocarbon Plus Fractions.*

[28] *Characterizing Hydrocarbon Plus Fractions.*

[29] *Characterizing Hydrocarbon Plus Fractions.*

[30] *Encyclopedia of Chemical Processing and Design. 62*

[31] *Conversion Process*.

[32] *Encyclopedia of Chemical Processing and Design.* 27

[33] *Petroleum Handbook*

[34] *Conversion Process*.

[35] *Conversion Process*.

[36] *Conversion Process*.

[37] *Conversion Process*.

[38] *Conversion Process*.

[39] *Conversion Process*.

[40] *Conversion Process*.

[41] *Properties of gases and liquids, the.* Reid, Robert C.

[42] Burisan, N.R., N.K. Volnukhina, A.A. Polyakov, and I.S. Fuks. *Kinetic relationships in the low-temperature isomerization of n-butane.* Khimiya i Teckhnologiya Topliv i Masel. No. 10, pp. 6-8, October, 1972.

[43] Aleksandrov, A.S. et al. *Kinetics of low-temperature n-pentane isomerization over NIP-66 catalyst.* Khimiya i Teckhnologiya Topliv i Masel. No. 10, pp. 5-8, October, 1976.

[44] Aleksandrov, A.S. et al. *Kinetics of low-temperature n-pentane isomerization over NIP-66 catalyst.* Khimiya i Teckhnologiya Topliv i Masel. No. 10, pp. 5-8, October, 1976.

[45] *Encyclopedia of Chemical Processing and Design.* 27

[46] Cheng-Lie Li, Zhe-Lin Zhu. *Network of n-Hexane isomerization over Pt/Al_2O_3 and Pd/HM catalysts.* Fuel Science and Technology Int'L. v. 9 n. 9. Jan. 01 1991 pg 1103-1122.

[47] Cheng-Lie Li, *Network*

[48] Gary and Handwerk

[49] Hydrocracking PFD, www.isa.org

[50] Meyers, Robert A. Handbook of Petroleum Refining Processes. 3rd edition. McGraw-Hill: NewYork, 2004, 14.35.

[51] Nelson, W.L. Oil and Gas Journal. 65 (26) 84-85 (1967).

[52] Nelson, W.L. Oil and Gas Journal.

[53] Nelson, W.L. Oil and Gas Journal.

[54] Firoozabadi, A., and Katz, D. L. 1978. Predicting phase behavior of condensate/crude-oil systems using methane interaction coefficients. Journal of Petroleum Technology 30(11):1649–1655.

[55] Firoozabadi, A., and Katz, D. L.

[56] Stangeland, B. E., "Kinetic Model for Prediction of Hydrocracker Yields," Znd. Eng. Chem. Proc. Des. Deu., 13(1), 72 (1974).

[57] C. S. Laxminarasimhan, R. P. Verma, P. A. Ramachandran. Continuous lumping model for simulation of hydrocracking. AIChE Journal. 42(9) 2645-2653 (1996).

[58] Solvent Dewaxing. Oil and Gas Journal. April 3, 1961. page 127.

[59] Krishna, R., G. C. Joshi, R. C. Purohit, K. M. Agrawal, P. S. Verma, S. Bhattacharjee Correlation of pour point of gas oil and vacuum gas oil fractions with compositional parameters. *Energy & Fuels*, 3(1) 15-20 (1989).

[60] Krishna, R., G. C. Joshi, R. C. Purohit,

[61] Firoozabadi, A., and Katz, D. L.

[62] Moulton, R.W. and V.K. Loop. Compostion of Petroleum Waxes from western crudes. Petroleum Refiner, 24(4) 121-3 (1945).

[63] May 4, 2006. http://www.prod.exxonmobil.com/refiningtechnologies/pdf/AlkyforWR02.pdf

[64] Alkylation of Isobutane with C3-C5 Olefins: Feedstock Consumption, Acid Usage, and Alkylate Quality for Different Processes Albright, L. F. Ind. Eng. Chem. Res.; (Article); 2002; 41(23); 5627-5631

[65] May 4, 2006. http://www.prod.exxonmobil.com/refiningtechnologies/pdf/AIChE2002SpringAlky.pdf

[66] Alkylation of Isobutane

[67] Alkylation of Isobutane with C3-C5 Olefins To Produce High-Quality Gasolines: Physicochemical Sequence of Events Albright, L. F. Ind. Eng. Chem. Res.; (Article); 2003; 42(19); 4283-4289.

[68] Alkylation of Isobutane

[69] The kinetics of alkylation of isobutane with propylene AIChE Journal Volume 18, Issue 4, Date: July 1972, Pages: 698-705 J. Randolph Langley, Ralph W. Pike

[70] Alkylation of Isobutane with C3-C5 Olefins To Produce High-Quality Gasolines: Physicochemical Sequence of Events Albright, L. F. Ind. Eng. Chem. Res.; (Article); 2003; 42(19); 4283-4289.

[71] Alkylation of Isobutane with C3-C5 Olefins To Produce High-Quality Gasolines: Physicochemical Sequence of Events Albright, L. F. Ind. Eng. Chem. Res.; (Article); 2003; 42(19); 4283-4289.

[72] Interfacial Area of Dispersions of Sulfuric Acid and Hydrocarbons David J. Ende, Roger E. Eckert, Lyle F. Albright Ind. Eng. Chem. Res.; 1995; 34(12); 4343-4350.

[73] Gary, J.H. and G.E. Handwerk. Petroleum Refining: Technology and Economics. Marcel Dekker Inc: New York, 2001, 121-141. and A.V. Mrstik, K.A. Smith, and R.D. Pinkerton, Advan. Chem. Ser. 5 ,97. 1951.

[74] A.V. Mrstik,

[75] A.V. Mrstik

[76] Gary, J.H. and G.E. Handwerk

[77] May 4, 2006. http://jechura.com/ChEN409/11%20Alkylation.pdf CO School of Mines

[78] Tabak, S.A., U.S. Patent 4,254,295 (1981)

[79] Conversion of propylene and butylene over ZSM-5 catalyst AIChE Journal Volume 32, Issue 9, Date: September 1986, Pages: 1526-1531 S. A. Tabak, F. J. Krambeck, W. E. Garwood

[80] Conversion of propylene and butylene over ZSM-5 catalyst

[81] Conversion of propylene and butylene over ZSM-5 catalyst

[82] Conversion of propylene and butylene over ZSM-5 catalyst

[83] Conversion of propylene and butylene over ZSM-5 catalyst

[84] LIQUID PROPANE Use in Dewaxing,Deasphalting, and Refining Heavy Oils Robert E. Wilson, P. C. Keith, , Jr. R. E. Haylett Ind. Eng. Chem.; 1936; 28(9); 1065-1078.

[85] Phase equilibria in supercritical propane systems for separation of continuous oil mixtures Maciej Radosz, Ronald L. Cotterman, John M. Prausnitz Ind. Eng. Chem. Res.; 1987; 26(4); 731-737.

[86] *May 4, 2006. http://www.scielo.br/scielo.php?script=sci_arttext&pid=S0104-66322000000300012&lng=pt&nrm=iso - PDF*

[87] Phase equilibria in supercritical propane systems for separation of continuous oil mixtures

[88] LIQUID PROPANE

[89] Asphalt flocculation and deposition: I. The onset of precipitation AIChE Journal Volume 42, Issue 1, Date: January 1996, Pages: 10-22 Hossein Rassamdana, Bahram Dabir, Mehdi Nematy, Minoo Farhani, Muhammad Sahimi

[90] Asphalt flocculation and deposition:

[91] Asphalt flocculation and deposition:

[92] Phase equilibria in supercritical propane systems for separation of continuous oil mixtures

[93] Phase equilibria in supercritical propane systems for separation of continuous oil mixtures

[94] Hagelberg, P. et. al. Kinetics of catalytic cracking with short contact times, Applied Catalysis A: General 223 (2002) 73-84

[95] Weekman, Vern W. Jr., Lumps, Models, and Kinetics in Practice, The American Institute of Chemical Engineers 1979, No. 11, Vol 75.

[96] (http://www.plantech.or.kr/diagram/pc_refinery/refinery_t2.gif)

[97] Weekman

[98] Juarez-Ancheyta, Jorge, et. al. Estimation of Kinetic Constants of a Five-Lump Model for Fluid Catalytic Cracking Process Using Simpler Sub-models, Energy & Fuels 2000, 14, 1226-1231

[99] Upson, L. Lawrence and Reagan, William J., et. al. The Art of Evaluating Laboratory Fixed Bed and Fixed Fluid Bed Catalytic Cracking Data, unpublished, January 2005

[100] Juarez-Ancheyta 2000

[101] Han, In-Su, Dynamic modeling and simulation of a fluidized catalytic cracking process. Part I: Process modeling, Chemical Engineering Science 56 (2001) 1951-1971

[102] Juarez-Ancheyta 2000

[103] Juarez-Ancheyta 2000

[104] Juarez-Ancheyta 2000

[105] Gary and Handwerk, 166

[106] Riazi, M.R. Characterization and Properties of Petroleum Fractions. West Conshohocken, PA: ASTM International, 2005., p. 335

[107] Riazi, p. 335

[108] Riazi, p. 335

[109] Riazi, p. 335

[110] Riazi, p. 335

[111] Riazi, p. 137

[112] Riazi, p. 137

[113] Riazi, p. 135

[114] Riazi, p. 135

[115] Riazi, p. 136

[116] Riazi, p. 135

[117] Riazi, p. 135

[118] Riazi, p. 138

[119] Riazi, p. 138

[120] Pongsakdi, Arkadej, et. al. Financial Risk Management in the Planning of Refinery Operations. *International Journal of Production Economics.* Accepted for publication, 20 April 2005.